GENE LOCALIZATION STUDIES IN TWO NEUROLOGICAL DISORDERS

by

Nadire Duru

B.S., Molecular Biology and Genetics, Istanbul Technical University, 2004

Submitted to the Institute for Graduate Studies in
Science and Engineering in partial fulfillment of
the requirements for the degree of
Master of Science

Graduate Program in Molecular Biology and Genetics
Boğaziçi University

2006

ACKNOWLEDGEMENTS

I would like to deeply thank to my thesis supervisor Prof. Aslı Tolun for her consistent and constructive help, guidance and criticism during this study. I feel very lucky for getting the chance to study with her.

I owe my appreciation to the members of my thesis committee, Assoc. Prof. Esra Battaloğlu and Prof. Nihan Erginel Ünaltuna for allocating their time to evaluate this work.

I would like to thank to NHLBI Mammalian Genotyping Service (Contract Number HV48141) for performing genome scan of the families.

I would like to thank to my group friends Sibel Aylin Uğur, Ayşe Cörüt and Murat Çetinkaya. The positive and sincere environment of this lab was a great support for me. I especially would like to thank to Sibel Aylin Uğur for her endless help and friendship in every day of these two years. This thesis would not have been completed without her.

I'm very grateful to my friends for their support and making these two years enjoyable. I especially thank to Demet Candaş and Kader Çavuşoğlu for being such great friends.

I would also like to thank to my family for the support and encouragement I received throughout my education. I'm very lucky for having a great family.

ABSTRACT

GENE LOCALIZATION STUDIES IN TWO NEUROLOGICAL DISORDERS

Autozygosity mapping is a frequently used powerful method for discovering loci for autosomal recessive diseases resulting from consanguineous marriages. Gene localization is an initial step for the identification of genes responsible for such disorders. Identification of a disease gene would enable us to better understand its functions, investigate the underlying cellular mechanisms, and provide critical insights into the pathogenesis of the disease. It can also improve the drug development and enable diagnostic and prenatal genetic testing. Computer programs developed to analyze data obtained by such studies are very helpful in finding the most likely gene locus, supplying ease and speed to studies. In the framework of this study, autozygosity mapping was performed to identify the gene loci for two rare autosomal recessive disorders: early onset progressive encephalopathy with myoclonus and dystonia (PEMD) and infantile neuroaxonal dystrophy (INAD). Computer based parametric tests including two and multi-point lod score analyses were also performed to assess the significance of the linkage data generated by autozygosity mapping and further candidate locus evaluation.

The gene responsible for PEMD was localized to a maximum 3.26 Mb-interval on telomere of chromosome 16p. Among the 173 genes residing in the identified locus, 25 could be assigned as candidate genes.

For INAD, on the other hand, no significant genetic linkage to any locus could be detected.

ÖZET

İKİ NÖROLOJİK KALITSAL HASTALIKTA GEN LOKALİZASYONU ÇALIŞMASI

Homozigotluk haritalaması, akraba evliliği sonucunda ortaya çıkan nadir otozomal çekinik hastalık genlerinin yerlerinin saptanması için sıklıkla kullanılan güçlü bir yöntemdir. Bu yöntem hastalık genlerinin ortaya çıkarılmasının ilk adımıdır. Bir hastalık geninin tanımlanması ise o genin fonksiyonu ile ilgili hücresel mekanizmaların daha iyi anlaşılmasında bize yardımcı olur ve hastalığın oluşumunu kavramamıza olanak sağlar. Hastalık geninin saptanması ayrıca ilaç üretilmesine ve doğum öncesi ve sonrası genetik tanıya da olanak sağlayacaktır. Bu tür çalışmalardan elde edilen verilerin analizi için geliştirilen bilgisayar programları, en olası gen bölgesini işaret ederek çalışmalara kolaylık getirip hız kazandırmaktadırlar. Bu çalışma çerçevesinde iki nadir otozomal çekinik hastalığın (bebeklik çağı miyoklonus ve distoni ile seyreden progresif ensefalopati ile infantil nöroaksonal distrofi) gen lokuslarını belirlemek amacıyla homozigotluk haritalaması yöntemi uygulanmıştır. İki ve çok noktalı lod skor analizini içeren bilgisayar destekli parametrik testler uygulanarak, bu hastalıkların homozigotluk haritalaması yöntemi sonucu elde edilen bağlantı bilgileri değerlendirilmiştir.

Bu çalışmada, PEMD hastalığından sorumlu gen 16. kromozomda, telomerden itibaren 3.26 Mb'lık bir bölgeye sınırlandırılmıştır. Bölgede bulunan 173 genin 25 tanesi aday gen olarak belirlenmiştir.

INAD hastalığından sorumlu genin lokalizasyonu için yürütülen çalışmalar sonucu ise, herhangi bir lokusa genetik bağlantı belirlenememiştir.

TABLE OF CONTENTS

LIST OF FIGURES

LIST OF TABLES

LIST OF ABBREVIATIONS

A	Adenine
AAA	ATPases associated with various cellular activities
ABAT	4-Aminobutyrate aminotransferase
APS	Ammonium peroxodisulphate
bp	Base pair
C	Cytosine
cM	Centimorgan
CoA	Coenzyme A
ddNTP	Dideoxynucleoside triphosphate
DMSO	Dimethyl Sulfoxide
DNA	Deoxyribonucleic acid
DRD2	D2 dopamine receptor
DYT1	Dystonia 1
DYT11	Dystonia 11
DYT15	Dystonia 15
EDTA	Ethylenediaminetetraacetate
EEG	Electroencephalogram
GABA	Gamma-aminobutyric acid
GABA-T	4-Aminobutyrate aminotransferase deficiency
G	Guanine
HO-1	Heme oxygenase 1
IBD	Identical by descent
INAD	Infantile Neuroaxonal Dystrophy
JP	Autosomal Recessive Juvenile Parkinsonism
Lod	Log of odds
Mb	Megabase
min	Minute
MLE	Maximum likelihood estimate
MLS	Maximum lod score
MRI	Magnetic Resonance Imaging

NBIA	Neurodegeneration with Brain Iron Accumulatin
PANK2	Pantothenate kinase 2 gene
PCR	Polymerase chain reaction
PD	Parkinson Disease
PKAN	Pantothenate kinase-associated neurodegeneration
PEMD	Early Onset Progressive Encephalopathy with Myoclonus and Dystonia
RFLP	Restriction fragment length polymorphism
rpm	Revolution per minute
SDS	Sodium dodecyl sulphate
SGCE	Epsilon-sarcoglycan gene
SNP	Single nucleotide polymorphism
SSTR5	Somatostatin receptor 5
T	Thymine
TEMED	N, N, N, N'-Tetramethylethylenediamine
U	Unit
VNTRs	Variable number tandem repeats
W	Watt

1. INTRODUCTION

In this study, genetic analyses were performed with the aim of identifying the gene loci of autosomal recessive neurological disorders Early Onset Progressive Encephalopathy with Myoclonus and Dystonia and Infantile Neuroaxonal Dystrophy.

1.1. Early Onset Progressive Encephalopathy with Myoclonus and Dystonia

The first disease studied in this thesis was early onset progressive encephalopathy with myoclonus and dystonia (PEMD). PEMD is a novel hereditary disorder, which is observed in a large Turkish inbred family and the clinical manifestations were evaluated by the neurologists collaborating in this study. It is inherited in an autosomal recessive pattern. The disease is early onset (by two months after birth) and has a steady progressive course. PEMD is characterized by myoclonic seizures, episodic phenomena as dystonia, alternating post-ictal enduring hemipareses, autonomic involvements, periods of obtundation, and lethargy. Developmental and neurological retardation together with systemic infections lead to a full deterioration, affecting the motor, mental and vital functions. The disease eventually leads to death within the first decade of life. The phenotypic features found to be unique for each patient included startling phenomena and restricted areas of discoloration on the skin and irregularities in respiration. Increase in the cranial imaging abnormalities in time, the slowing of the background activity and the disappearance of phasic elements of sleep in the subsequent EEGs support the progressive course of the disease.

The clinical picture supported by EEG and imaging findings suggested a genetically determined degenerative disease with some unique characteristics and without close resemblance to any previously well-known condition. Although the metabolic tests were not informative to allow a specific diagnosis, the condition was considered to be due to an inborn error of metabolism.

Inborn errors of metabolism appear in general before birth, at birth, or during the first days of life as sudden death or as deterioration after normal birth and delivery

(Leonard and Morris, 2000). Metabolic disorders could cause neurological disease, including infantile epilepsy. However, it is not easy to clearly characterize seizures and epilepsy syndromes. This prevents the recognition of features suggestive of specific underlying metabolic and neurodegenerative etiologies. In particular, myoclonic seizures in infancy suggest an inborn error of metabolism. Moreover, there are some epileptic syndromes known to be associated with metabolic disorders including some forms of neonatal seizures, West's syndrome, early myoclonic encephalopathy and early infantile epileptic encephalopathy (Nordli and De Vivo, 2002). Among the several clinical criteria for suspecting the presence of an inborn error of metabolism are psychomotor retardation, intractable or myoclonic seizures, hypotonia and lethargy (Velázquez *et al.*, 2000), all of which are seen in the PEMD patients.

Two other diseases that have some common clinical features with PEMD are discussed below.

1.1.1. Myoclonic Dystonia

Myoclonic dystonia (MIM 159900) is a hereditary disease inherited as an autosomal dominant trait with incomplete penetrance and variable onset. Although the main clinical feature is dystonia, tremor or rapid jerky movements resembling myoclonus may also be present.

Three genes were found to be responsible for myoclonic dystonia. Myoclonic dystonia caused by mutation in the SGCE gene is known as DYT11. The disease was also found to be caused by mutations in the gene encoding D2 dopamine receptor (DRD2; 126450) and the gene encoding torsin-A (DYT1; 605204). In addition, locus 18p11 was found as a candidate region harboring the fourth gene responsible for yet another form of myoclonic dystonia (DYT15; 607488).

The *SGCE* gene at 7q21 encodes the epsilon member of the sarcoglycan family. The gene is the transmembrane component of the dystrophin-glycoprotein complex, which links the cytoskeleton to the extracellular matrix. Five heterozygous loss-of-function

mutations and two large heterozygous deletions in the gene were found to be associated with myoclonus dystonia (Zimprich *et al.*, 2001; Asmus *et al.*, 2002).

The *DRD2* gene encodes D2 dopamine receptor. The D2 dopamine receptor is a G protein-coupled receptor located on postsynaptic dopaminergic neurons that are centrally involved in reward-mediating mesocorticolimbic pathways. Receptors SSTR5 and D2R interact physically through heterooligomerization to create another receptor with enhanced functional activity (Rocheville *et al.,* 2000). Interaction of receptors from different G protein-coupled receptor families through oligomerization defines a new and more complex level of molecular crosstalk between related G protein-coupled receptor subfamilies. A missense mutation in the *DRD2* gene was found to be associated with myoclonic dystonia (Klein *et al.*, 1999).

The *DYT1* gene encodes Torsin-A, a member of the ATPases associated with various cellular activities (AAA). It has high expression in melanized neurons of the pars compacta of the substantia nigra, as well as in cerebellum, dentate gyrus and stratum pyramidal of CA3. A 3 bp deletion (Ozelius *et al.*, 1997) as well as a 18 bp deletion (Leung *et al.*, 2001) and a missense mutation (Klein *et al.*, 2002) in this gene were found to be associated with myoclonic dystonia.

1.1.2. 4-Aminobutyrate Aminotransferase Deficiency

4-Aminobutyrate aminotransferase deficiency (GABA-T, MIM 137150) is an inborn error of gamma-aminobutyric acid (GABA) degradation. GABA-T is a rare disease inherited as an autosomal recessive trait. The clinical characteristics of the disease include psychomotor retardation, hypotonia, hyperreflexia, lethargy, refractory seizures, accelerated growth, and electroencephalographic abnormalities (Jaeken *et al.*, 1984; Medina-Kauwe *et al.,* 1999).

The gene responsible for the disease was found to be *ABAT* gene, which was mapped to 16p13.3 by The International Radiation Hybrid Mapping Consortium. *ABAT* encodes the gamma-aminobutyrate transaminase that is directly responsible for the degradation of

GABA into succinic semialdehyde in the brain. GABA is an important and mostly inhibitory neurotransmitter in the central nervous system.

1.2. Infantile Neuroaxonal Dystrophy

The other disease studied in the framework of this thesis was Infantile Neuroaxonal Dystrophy (INAD, MIM 256600) or Seitelberger's Disease. It is a rare hereditary neurodegenerative disorder inherited as an autosomal recessive trait with onset in early childhood, generally by three years of age. The incidence of the disease is unknown. It is characterized by progressive motor and mental deterioration, bilateral pyramidal tract signs, development of hypotonia or low muscle tone and early visual disturbances such as strabismus, nystagmus, optic atrophy and visual loss. Some individuals with INAD have iron deposits in their brain. These symptoms may be accompanied by impaired hearing. The epileptic seizures and extrapyramidal symptoms are usually absent, or they appear as late features. The low muscle tone eventually leads to spastic tetraplegia, confining patients to bed or wheelchairs. Cerebellar atrophy is the most common finding at postmortem examination. Death usually occurs around the age of 10 years.

Skin, nerve, conjunctiva and rectum biopsies reveal the presence of axonal swellings and 'spheroid bodies' throughout the central and peripheral nervous systems, as a pathological hallmark of INAD.

Although the deficiency of a lysosomal enzyme, α-N-acetylgalactosaminidase, has been described in some patients with this disorder, in most of the cases the underlying metabolic defects remain unknown and the pathogenesis is unclear. Since the basis of the metabolic or genetic defect has not been identified yet, currently there is no effective treatment, and neither is prenatal diagnosis available.

The diagnostic criteria for INAD were first defined by Aicardi and Castelein (1979): onset of symptoms before three years of age, a clinical picture characterized by psychomotor degeneration, increased neurologic involvement with symmetric pyrimadial tract signs and marked truncal hypotonia, a relentlessly progressive course leading to spastic tetraplegia, blindness and dementia, and unequivocal histological evidence. Aicardi

and Castelein (1979) noted that clinical as well as pathologic features were necessary for diagnosis. Ozmen *et al.* (1991) demonstrated that the diagnosis could be made by ultrastructural examination of biopsied skin, and Seven *et al.* (2002) suggested that facial dysmorphism could permit diagnosis in the first months of life before any clinical or neurologic signs are evident.

Two diseases with similar clinical manifestations are described below.

1.2.1. Neurodegeneration with Brain Iron Accumulation

Neurodegeneration with Brain Iron Accumulatin (NBIA) is a rare inherited neurological movement disorder transmitted in an autosomal recessive fashion. It is characterized by the progressive degeneration of the nervous system, especially the globus pallidus and substantia nigra pars reticularis (Koeppen and Dickson, 2001). Dr. Hallervorden performed euthanasia for mentally ill patients during World War II, which is considered unethical today. Therefore, the name of this disease has been changed from Hallervorden-Spatz syndrome to Neurodegeneration with Brain Iron Accumulation (NBIA). The term NBIA is a general term, covering all conditions previously categorized as Hallervorden-Spatz syndrome (Gordon, 2002).

All individuals with NBIA have iron accumulation in brain along with a progressive movement disorder. They show variable symptoms, so the genetic cause may differ among families. It is highly possible that different genes are responsible for NBIA; furthermore, different mutations within the same gene could lead to more or less severe forms of the disease. The factors that influence disease severity and rate of progression are still unknown.

Common clinical features include mental deterioration, emaciation, severe feeding difficulties, visual impairment, dystonia, muscular rigidity, and sudden involuntary muscle spasms (spasticity). These features can result in clumsiness, walking problems, difficulty in controlling movement, and speech problems. Symptoms are progressive and become worse over time (Elejalde *et al.*, 1979).

Zhou *et al.* (2001), found that individuals with NBIA have mutations in *PANK2*, a gene that helps to metabolize vitamin B_5. The mutations included a 7-bp deletion and some missense and null mutations.

The largest subgroup of NBIA is Pantothenate Kinase Associated Neurodegeneration (PKAN, MIM 234200), an autosomal recessive disorder similar to INAD with overlapping clinical and pathologic features. The symptoms associated with classical or atypical PKAN cases are not the same. While individuals with classical disease display a rapid progression, atypical cases progress slowly, usually over several years. The symptoms vary also from case to case.

PKAN also is found to be associated with mutations in *PANK2* gene. Pellecchia *et al.* (2005) identified five novel mutations in the gene in PKAN patients. No genes have been identified for the other forms of NBIA.

Pantothenate kinase is a key regulatory enzyme in the synthesis of coenzyme A (CoA) from pantothenate, indicating that PKAN is the result of a defect of pantothenate metabolism. The enzyme catalyzes the cytosolic phosphorylation of pantothenate (vitamin B5), N-pantothenoylcysteine, and pantetheine. CoA is the major acyl carrier, playing a central role in fatty acid metabolism. In both yeast and fly, each with only one pantothenate kinase gene, the null mutant is inviable (Zhou *et al.*, 2001).

Hortnagel *et al.* (2003) determined the exon-intron structure of the human *PANK2* gene and identified two alternatively used first exons. The resulting transcripts encode distinct isoforms of *PANK2*, one of which carries an N-terminal extension with a predicted mitochondrial targeting signal.

INAD and NBIA have several features in common. In particular, pathological examination reveals axonal swelling and spheroid bodies in the central nervous system in both diseases. Since the first description of INAD, there has been a discussion whether these syndromes are distinct entities or the extremes of a disease spectrum. The fact that INAD and PKAN diseases have in common several clinical, radiological, and pathological features supported the hypothesis of an allelic relationship. However, haplotype analysis

of one consanguineous INAD family excluded linkage to *PANK2* gene. Furthermore, sequencing studies in seven other INAD families revealed no mutations in *PANK2* or in other genes of CoA biogenesis (Hortnagel *et al.*, 2004). Thus, it was concluded that INAD and PKAN are genetically distinct disorders (Nordocci, 2004).

Hortnagel *et al.* (2004) reported some of the phenotypic differences between INAD and PKAN. INAD onsets generally within the first two years, leading to death before age 10, whereas PKAN is late-infantile or juvenile onset, and patients may survive into third decade. However, there are reports of both early-infantile PKAN and late-onset INAD. INAD is characterized mainly by a pyramidal syndrome with spastic tetraplegia, hyperreflexia, and visual impairment, whereas PKAN is more of an extrapyramidal syndrome with dystonia, parkinsonism, and choreoathetosis. Both disorders have axonal swellings and spheroids throughout the central nervous system, but patients with INAD may also have spheroids in peripheral tissues. PKAN is associated with iron accumulation in the basal ganglia, leading to the characteristic 'eye of the tiger' sign on brain MRI. INAD shows cerebellar atrophy with hyperintensity in the cerebellar cortex. However, both imaging and pathologic features can show overlap in both diseases.

1.2.2. Autosomal Recessive Juvenile Parkinsonism

Parkinson disease (PD, MIM 168600) is a frequent autosomal dominant neurodegenerative disorder associated with degeneration of dopaminergic neurons in the zona compacta of the substantia nigra. Its onset is generally in the sixth decade of life. It is characterized by the presence of Lewy bodies, which are cytoplasmic eosinophilic hyaline inclusions. Although the genetic heterogeneity is likely, it has been suggested that genetic factors are effective in the etiology of PD. Although it shares several features with PD, such as bradykinesia, rigidity, and tremor, autosomal recessive juvenile parkinsonism (JP), which has an onset before age 40 is considered a different disease. JP was found to be caused by mutations in the parkin gene (*PARK2*) on chromosome 6q, which spans more than 500 kb and has 12 exons (Kitada *et al.*, 1998). It is expressed in neuronal processes and cell bodies of neurons, but not in glial cells, in the midbrain, basal ganglia, cerebral cortex, and cerebellum. Both diurnal fluctuation of symptoms and mild dystonia are common manifestations of JP. Both the pathology and pattern of inheritance in JP is

different from those in PD. Although pathological findings have shown that the affected brain regions in JP are similar to those in PD, Lewy bodies that are the hallmark of PD are absent in JP (Jones *et al.*, 1998 ; Periquet *et al.*, 2001).

A wide variety of mutations in the gene, including exon deletions and duplications, as well as point mutations, have been found to be associated with JP (Periquet *et al.*, 2001). Mutations in the gene were also found in PD patients, demonstrating that parkin mutations are not limited to juvenile onset. Parkin is composed of an ubiquitin-like domain in the N-terminus and two RING finger motifs toward the C-terminus. Several inactivating mutations have been found in the RING finger domains, suggesting that these domains are functionally important. Parkin is an ubiquitin ligase that ubiquitinates misfolded proteins targeted for the proteasome-dependent protein degradation pathway. Synaptotagmin XI has been identified as a protein that interacts with parkin. Parkin binds to C2A and C2B domains of synaptotagmin XI, resulting in the polyubiquitination of synaptotagmin XI. Truncated or missense mutated parkins reduce parkin-sytXI binding affinity and ubiquitination. The fact that parkin can directly interact with ubiquitinate synaptotagmin XI strongly implicates that parkin has a role in modifying synaptic vesicle trafficking at the presynaptic terminal. It can be speculated that the loss of parkin function in patients with JP increases synaptotagmin XI activity, resulting in increased dopamine release, which in turn causes dystonia and parkinsonism. Impaired vesicle functioning may cause an increase in cytoplasmic dopamine, resulting in increased oxidative damage and subsequently cell death, explaining the neurodegeneration seen in patients with parkin mutations (Doung *et al.*, 2003). Moreover, in a study it was demonstrated that iron staining in JP was more intense than in sporadic Parkinson's disease (PD), and there were differences in the pattern of distribution of iron between JP and PD. Thus, it was postulated that oxidative stress may play an important role in the neurodegeneration associated with JP. The relation of parkin protein abnormality to iron accumulation is not known; however, there are three speculations. The RING-finger-like motif of the parkin protein may bind iron, causing it to accumulate in the cytoplasm in the absence of normal parkin protein. Secondly, if the parkin protein is involved in the vesicular transport system, lack of the protein may lead to excess deposition of free dopamine and oxidized proteins in neurites and cytoplasm and eventually accumulation of iron. Free dopamine releases free iron from ferritin. Also, dopamine upregulates heme oxygenase-1 (HO-1), which

increases cellular levels of heme-derived free iron. Thirdly, the degree of iron accumulation may be determined by the length of time from the onset of the illness to death (Takanashi *et al.*, 2001).

1.3. Genetic Linkage

Genetic maps are used to find genes associated with genetic diseases. For most diseases, the location of the gene responsible is not known. Genetic maps are very useful for determining the rough location of a gene, since they make much easier to navigate the chromosomes. Once the rough location of the gene is determined, it is much easier to find out which of the genes at the locus is the actual disease gene. Linkage analysis often relies on the use of genetic markers that are closely located along the chromosome for estimating the location of a gene responsible for a disease within a relatively narrow length of DNA.

Genetic linkage analysis, which was first developed by the British geneticists William Bateson and Reginald Punnett, is used to discover the location of genes. Genetic linkage involves the estimation of the distances between genetic loci, which is achieved by using the fact that genes lying close to each other on a chromosome tend to be inherited together. The closer the genes are the higher is the probability to be inherited together. During meiosis the recombination can separate even closely linked genes, but the general rule is that for genes located on the same chromosome, the probability of a crossover event which creates recombination between two genes is directly related to the distance between them. Thus, the approximate distance between two genes can be determined by calculating the recombination frequency between them. Recombination frequency, denoted by θ, is the frequency or probability that crossover will take place between two loci (or genes) during meiosis. Since recombination frequency is a measure of genetic linkage, it has been used to develop genetic or linkage maps. To generate a complete genetic map of a chromosome, a large number of markers are used for genotyping in several families, and complex statistical analyses are employed to compare the inheritance across all markers.

The unit of recombinant frequency is the centimorgan (cM), termed in the name of geneticist Thomas Hunt Morgan. One cM is equal to a one per cent probability that two markers will be separated from each other due to a crossing over in a single meiosis. In

other words, two loci showing one per cent recombination are one cM apart from each other on the genetic map. The centimorgan is not a measure of physical distance. Typically, a genetic distance of one cM corresponds to a physical distance of roughly one million base pairs of DNA.

Linked genes have a recombination frequency that is less than 50 per cent ($\theta < 0.5$). When two genes are close together on the same chromosome, they do not assort independently and are said to be linked. As a consequence of independent assortment, the recombinant frequency will always be 50 per cent ($\theta = 0.5$) when two genes are located on different chromosomes.

There are some complications in the analysis of recombination events. The first complication arises from the fact that the further apart two loci are, the more likely it is that two or more recombination events could occur between them. When two recombination events occur, it seems as if no such event has occurred due to the shuffling and reshuffling of the alleles back to the way they were. The second complication arises from the fact that the occurrence of one recombination event on a chromosome tends to inhibit the occurrence of a second recombination event, especially in regions close to the first one. This is called "interference" and will generally make the map smaller. To take into consideration this fact, "map functions" have been created that are used to better estimate the true recombination distance between two markers.

Map functions are mathematical equations that are based on assumptions about how much recombination and interference exist on a chromosome. Map function distances are measured in centimorgan units. Two widely used map functions are the Haldane map function, which assumes that there is no interference between loci and the crossovers are random and independent, and the Kosambi map function, which assumes a moderate level of interference assuming that crossovers cannot occur very close to each other. Thus, the recombination fraction is modified by the map function. Computer programs such as MAPFUN (Keats *et al.*, 1989) can perform such modifications. Generally for genetic distances up to about 10 per cent recombination, one per cent recombination roughly equals to one cM. There are two main approaches for linkage analysis which are parametric (or model based) and nonparametric (or model-free) methods. Unlike the

nonparametric ones, parametric linkage analyses require specification of genetic parameters describing the disease gene transmission model including penetrance, as well as disease-allele frequency, phenocopy and mutation rates. In large pedigrees, the segregation of the putative gene responsible for the disease and the genetic markers with known loci is determined to localize the disease gene with respect to the known position of the linked genetic marker.

Lod (**l**og of **od**ds) Score analysis developed by Newton E. Morton is a powerful statistical method that facilitates the estimation of the genetic distance or at least the closeness between the putative disease locus and polymorphic markers. Moreover, since lod scores are logarithmic, lod scores for a particular trait from different families can be added together.

Lod score analysis is based on the comparisons of likelihoods for specific genetic linkage hypotheses, which are the alternative hypothesis of linkage specified by various values of the recombination fraction less than 0.50 and the null hypothesis of no linkage specified by $\theta = 0.50$.

For ease of comparison, the base 10 logarithm of the odds ratio is reported. Lod score, denoted by the function $Z(\theta)$, is calculated at several values of θ and the maximum test statistics of Z-maximum likelihood lod score (MLS) is reported. The maximum likelihood estimate (MLE) is the θ value which is the largest value of the MLS (Ott, 1991).

Two-point computerized lod score analysis is an efficient method to analyze for linkage complex pedigrees with mendelian traits. As a result of the analysis, a table of lod scores at various recombination fractions is obtained, and a curve can be plotted. A region with a lod score greater than 3.0 corresponds to an odds ratio of 1000 to 1 and is taken as evidence for linkage, and those with lod scores of less than –2.0, meaning an odds ratio of less than one in 100, is taken as evidence against linkage and are excluded (Pauls, 1999). Lod score values between –2.0 and 3.0 are inconclusive (Nyholt, 2000).

Multi-point computerized lod score analysis is even more powerful than two-point lod score analysis. It is based on the simultaneous analysis of the data for more than 2 loci.

It helps overcome limited informativeness of markers. The mapping function and the exact distances between markers modify the value of the lod score. The highest peak on the curve indicates the most likely location.

Although standard lod score analysis is a very powerful method for locating a disease gene, it is not without problems. First of all, it is vulnerable to errors, which can generate spurious recombinants. Additionally, computational limits on large pedigrees to be analyzed, limits on the resolution of the genetic mapping and problems with locus heterogeneity create difficulties. Also, a precise genetic model, involving the mode of inheritance, gene frequencies and penetrance of each genotype need to be specified.

1.3.1. Genetic Markers

The genome projects intend to construct high-resolution physical and genetic maps prior to obtaining the ultimate physical map. Genetic mapping depends on genetic markers spaced at intervals no greater than about 20 cM throughout the genome. In order to construct a genetic map with high resolution, the markers should be highly polymorphic, which makes them more informative, and they should be easily and reliably genotyped.

Restriction fragment length polymorphisms (RFLPs) were the first generation of DNA markers. They are based on the presence or absence of a target for a restriction enzyme, usually due to the polymorphism at a single base pair. They span the genome with a spacing of more than 10 cM (Donis-Keller *et al.*, 1987). The main problem with RFLPs was that by definition there can be only two alleles at a locus. So, they have limited informativeness, and the maximum heterozygosity they yield is 0.5. Nevertheless, they had a great impact on human genetic research in the 1980s.

Minisatellite Variable Number Tandem Repeats (VNTRs) are short nucleotide sequences ranging from 14 to 100 nucleotides long and composed of tandem repeats clusters. They were more useful as markers, because they are multiallelic. They have, therefore, high heterozygosity, and most meioses are informative. However, they also have their drawbacks. The large number of repeats in the locus cannot be amplified easily by

Polymerase Chain Reaction (PCR), and VNTRs are not evenly distributed throughout the genome but are clustered near the telomers.

Microsatellite markers are repeats of two to five nucleotides. They overcome the limitations of minisatellite markers, since they are more abundant and more evenly distributed.Moreover, they are highly polymorphic and easy to assay. These properties make the microsatellite markers the basis for the second-generation linkage map of the human genome (Weissenbach *et al.*, 1992). Murray *et al.* (1994) constructed a mostly microsatellite based map with one cM resolution.

The newest generation of markers is the two-allelic single nucleotide polymorphisms (SNPs). They include the classic RFLPs and also other single nucleotide polymorphisms that do not create or abolish a restriction site. Although they have limited informativeness, the advantages of SNPs are that they can be assayed on solid-state arrays without the aid of gel electrophoresis and they are often in clusters.

1.3.2. Autozygosity Mapping

The term autozygosity is used to indicate that two homologous chromosomal regions in an individual are identical by descent (IBD), i.e., both copies of a gene at the locus are derived from the same ancestor. Persons in consanguineous families with rare recessive diseases are likely to be autozygous for markers linked to the disease locus. Autozygosity mapping is a frequently used method for discovering autosomal recessive disease loci. The method is based on the fact that the affected individuals for an autosomal recessive trait who have consanguineous parents most likely have received the disease locus in the homozygous state identical by descent, from a common ancestor (Lander and Botstein, 1987). Searching for common homozygous regions shared by such individuals by using autozygosity mapping is a highly effective method for mapping loci, an initial step for the identification of genes responsible from autosomal recessive disorders (Forshew and Johnson, 2004). The identification of such genes enables diagnostic and prenatal testing. It can also provide critical insights into the pathogenesis of the disease and can improve drug development.

Consanguineous matings contribute to genetic studies by increasing the incidence of autosomal recessive disorders. Closely related individuals have a higher chance of carrying the same defective alleles than unrelated individuals; therefore, the offspring of consanguineous parents are more frequently homozygous for disease alleles than those from other unions. Generally the frequency of a trait is so low that the disease can only arise due to consanguinity, and in such cases, it is very probable that the affected individuals in the population are all homozygous by descent.

Inbred families are of great value for linkage studies since even small inbred families can generate significant lod scores (Doeblin, 1985). In order to identify loci harboring genes responsible for autosomal recessive disorders by using autozygosity mapping, suitable families may be found in Middle Eastern countries where the incidence of consanguineous marriages are high (Doeblin, 1985). For instance, in the Anatolian population, it has been estimated that 21 per cent of the marriages are consanguineous, with first-cousin marriages as the most common type. In the eastern and southern regions of Anatolia, inbreeding rate was found to be highest (Başaran *et al.*, 1998). Furthermore, the autozygosity mapping method is found to be effective for diseases which show great locus heterogeneity whenever large inbred families are present, such as in locating the genes for autosomal recessive nonsyndromic hearing loss (Guilford *et al.*, 1994).

1.3.3. Computer Based Linkage Programs

The computerized programs used in the context of the study are given in Table 1.1.

Table 1.1. Computer based linkage programs and their descriptions.

Program Name	Description	Reference
LINKAGE	Computations for genetic linkage analysis. Calculation of both two/multi-point lod scores, MLE of recombination fractions and genetic risks.	Lathrop *et al.*, 1984; Terwilliger and Ott, 1994
FASTLINK	FASTLINK is a significantly modified and improved version of the main programs of LINKAGE. It is roughly one order of magnitude faster than LINKAGE on long runs.	Cottingham *et al.*, 1993
GENEHUNTER	Rapid extraction of complete multipoint inheritance information from pedigrees of moderate size. Quick calculations involving dozens of markers, even in pedigrees with inbreeding and marriage loops, is possible.	Kruglyak *et. al.,* 1996
SimWalk2	A statistical genetics computer application for haplotype, parametric linkage, non-parametric linkage (NPL), identity by descent (IBD) and mistyping analyses on *any size* of pedigree.	Sobel and Lange, 1996 Sobel *et al.,* 2001 Sobel *et al.,*2002
PEDCHECK	A program for the detection of marker typing incompatibilities in pedigree data. Having four levels for error detection, it uses the individual's genotypes as given in the pedigree to check for inconsistencies between parents and offspring.	O'Connell and Weeks, 1998

2. PURPOSE

The purpose of this study was to identify candidate loci for two autosomal recessive neurological disorders Early Onset Progressive Encephalopathy with Myoclonus and Dystonia and Infantile Neuroaxonal Dystrophy. The initial genome scan had been performed by NHLBI Mammalian Genotyping Service (Contract Number HV48141). The aim was to evaluate the initial data for candidate loci and perform further genotyping at those loci for the purpose of assessing whether any of them could be the locus harboring the gene responsible for the relevant disease. To achieve these goals, homozygosity mapping strategy was employed by using polymorphic markers, and computer programs developed for parametric linkage tests were utilized to assess the significance of the data obtained.

3. MATERIALS

3.1. Blood Samples

Peripheral blood samples from patients with PEMD and their family members used in this study were provided by Dr. Nilgün Selçuk at Pediatric Clinic, Haseki Training and Research Hospital in İstanbul.

Peripheral blood samples from INAD patients and their family members used in this study were provided by Dr. Davut Gül at the Military Academy of Medicine in Ankara, Dr. Beyhan Tüysüz at Cerrahpaşa Medical School in İstanbul and Mehmet Seven at Istanbul University Cerrahpasa Medical School, Genetics and Teratology Application and Research Center in İstanbul.

3.2. Families

A large inbred Turkish family with five individuals afflicted with PEMD was studied. The pedigree of the family is given in Figure 3.1. The parents of the affected individuals were either blood relatives or originated from the same or neighboring villages. Blood samples from a total of 33 subjects including three affected individuals and the parents of two others were available. Those individuals are marked in Fig.3.1. An initial genome scan had been performed by NHLBI Mammalian Genotyping Service (Contract Number HV48141) as a service grant using DNA samples of 26 individuals. A total of 400 microsatellite markers with an average spacing of eight cM were used. The genotyped individuals are marked in the pedigree (Fig.3.1).

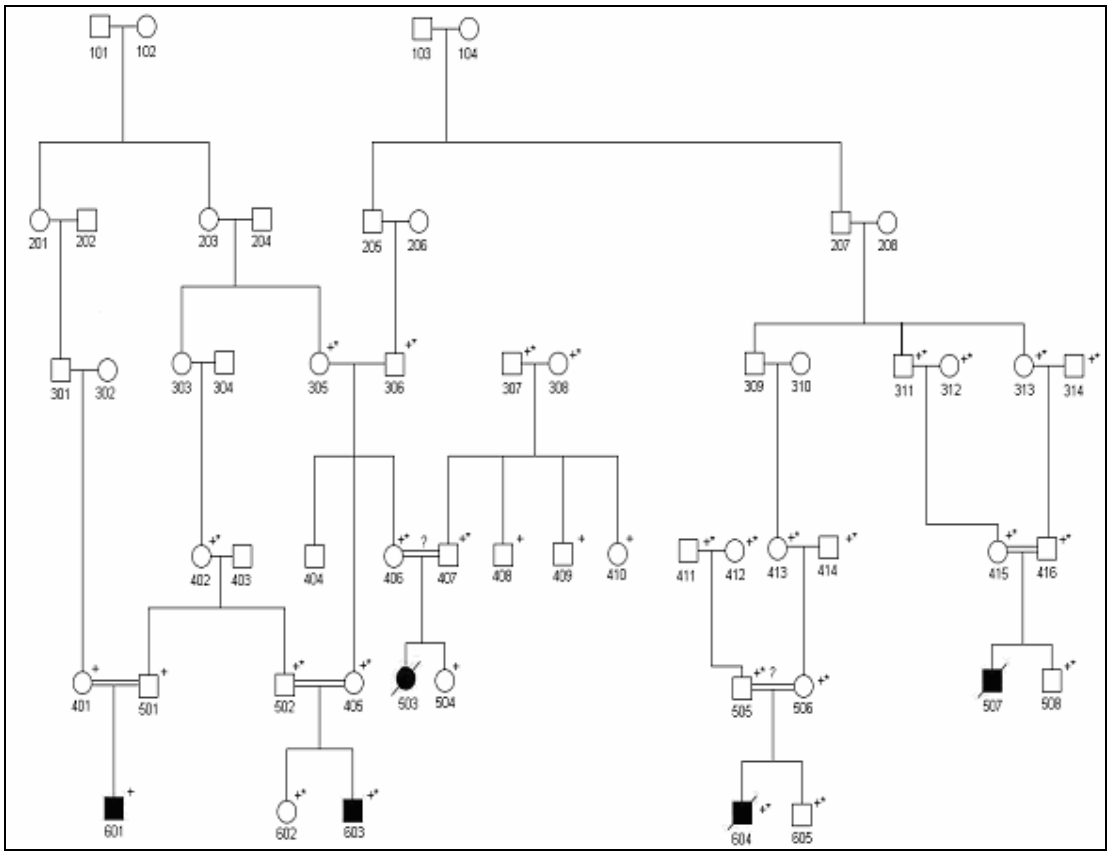

Figure 3.1. Pedigree of PEMD family. Plus sign indicates that DNA was available from the individual. Asterisk sign indicates that an initial genome scan had been performed

There were five families who were afflicted with INAD and available for study. DNA samples from 13 members of Family 1, including the two affected ones had been collected for study. Family 2 had seven healthy and two affected individuals. Family 3 was not suitable for linkage study, since it was small with only one affected individual. Family 4 was also small but with two affected individuals. Family 5 had one deceased affected individual from whom DNA sample had not been obtained. An initial genome scan was previously done in our laboratory (Akyüz, 2002). The polymorphic markers employed in the scan were in the set MapPairs version 8a (Research Genetics, USA). The set contained 156 markers that spanned the autosomes with an average spacing of 25 cM. Another genome scan had been performed by NHLBI Mammalian Genotyping Service (Contract Number HV48141) as a service grant using DNA samples from families 1, 2 and 3. A total of 400 microsatellite markers with an average spacing of eight cM had been used. Figure

3.2 shows the pedigree of INAD Family 1 and Figure 3.3 shows the pedigrees of INAD families 2, 3, 4 and 5. The genotyped individuals are marked in the pedigrees.

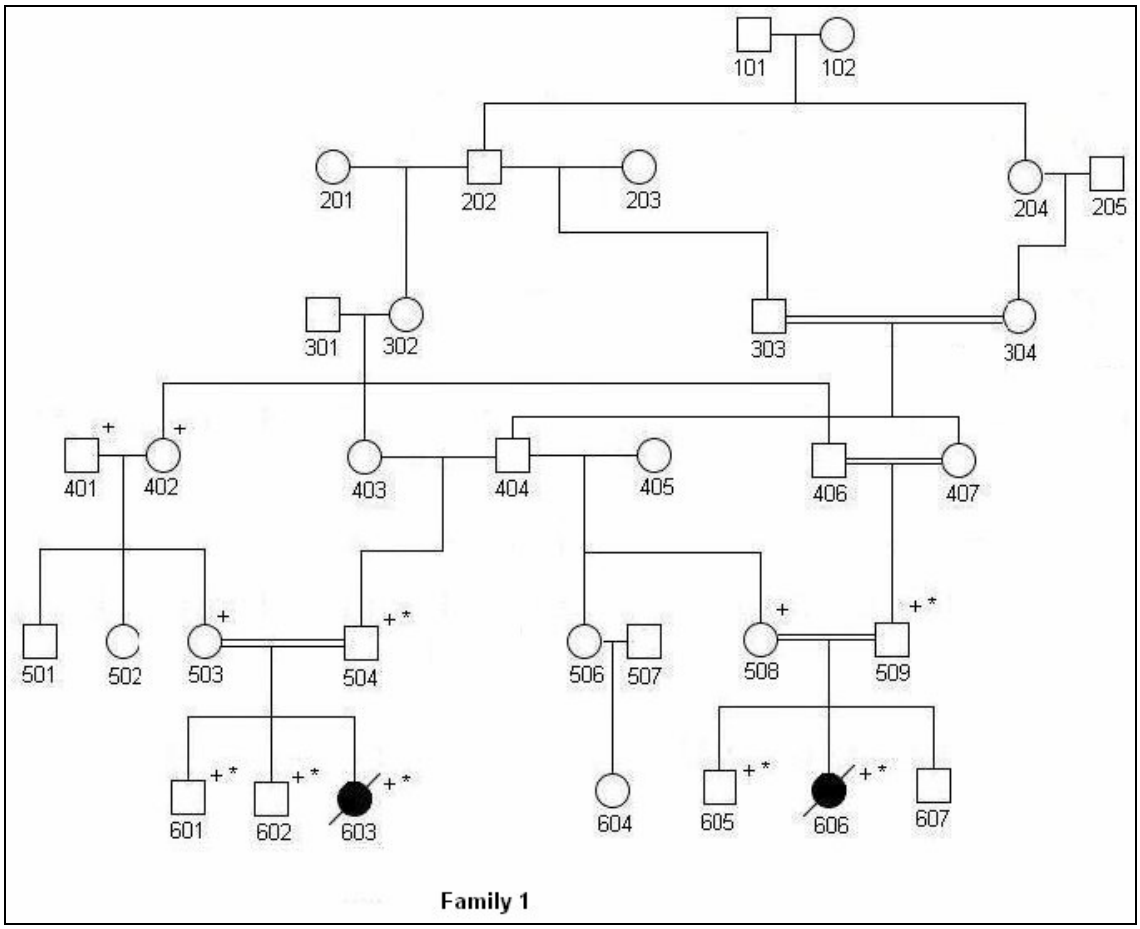

Figure 3.2. Pedigree of INAD family 1. Plus sign indicates that DNA was available from the individual. Asterisk sign indicates that an initial genome scan had been performed

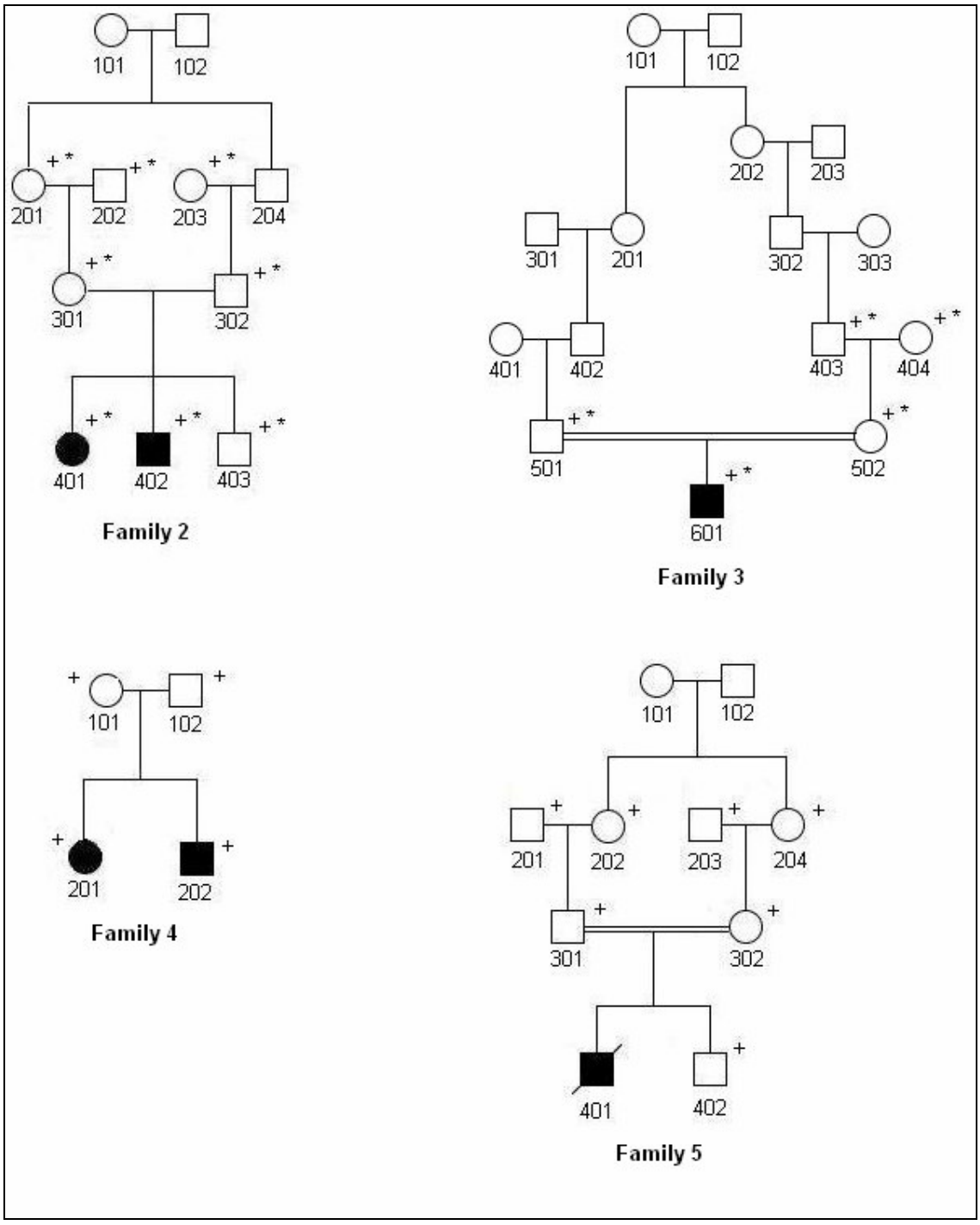

Figure 3.3. Pedigrees of INAD families 2, 3, 4 and 5. Plus sign indicates that DNA was available from the individual. Asterisk sign indicates that an initial genome scan had been performed

3.3. Chemicals

All chemicals used in this study were purchased from MERCK (Germany) or Sigma (USA), unless stated otherwise in the text.

3.4. Buffers And Solutions

3.4.1. DNA Extraction from Peripheral Blood

Cell Lysis Buffer	:	155 mM NH_4Cl, 10 mM $KHCO_3$ 0.1 mM Na_2EDTA (pH 7.4)
Nucleus Lysis Buffer	:	400 mM NaCl, 2 mM Na_2EDTA, 10 mM Tris (pH 8.2)
Proteinase K	:	20 mg/ml Proteinase K in dH_2O (Promega, USA)
Sodiumdodecylsulfate (SDS)	:	10 per cent SDS (w/v) in dH_2O
Ammonium Acetate	:	7.5 M CH_3COONH_4 in dH_2O
Ethanol	:	Absolute Ethanol (Carlo-Erba, Germany)
TE buffer	:	1 mM EDTA, 20 mM Tris-HCl, pH 8.0

3.4.2. Polymerase Chain Reaction (PCR)

10 X PCR Buffer	:	15 mM $MgCl_2$, 500 mM KCl, 100 mM Tris-HCl, pH 8.3
$MgCl_2$	:	25 mM $MgCl_2$ (Promega, USA)

dNTP	:	12.5 Mm each of dATP, dCTP, dGTP and dTTP in dH_2O
Betaine	:	5 M Betaine (Promega, USA)
Formamide	:	1.24 per cent Formamide
DMSO	:	8 per cent DMSO
Glycerol	:	10 per cent glycerol

3.4.3. Agarose Gel Electrophoresis

Agarose	:	2 per cent Agarose in 0.5 X TBE buffer
10 X TBE Buffer	:	20 mM EDTA, 0.89 M Boric Acid, 0.89 M Trizma base (pH 8.3)
10 X Loading Buffer	:	2.5 mg/ml Xylene Cyanol in Glycerol
Ethidium Bromide	:	20 mg/ml in dH_2O

3.4.4 Denaturing Polyacrylamide Gel Electrophoresis (PAGE)

40 per cent Acrylamide (Stock)	:	40 per cent Acrylamide-bisacrylamide (19:1) in dH_2O
8 per cent Instagel (Denaturing)	:	8 per cent Acrylamide-bisacrylamide (19:1), 8.3 M urea in 1 X TBE buffer
12 per cent Instagel (Denaturing)	:	12 per cent Acrylamide-bisacrylamide (19:1), 8.3 M urea in 1 X TBE buffer
APS	:	10 per cent Ammonium Peroxidisulfate

TEMED	:	N,N,N,N-tetramethylethylenediamine
10 X Sample Buffer	:	95 per cent formamide, 20 mM EDTA, 0.05 per cent xylene cyanol, 0.05 per cent bromophenol blue

3.4.5. Silver Staining

Staining Buffer (Buffer B)	:	0.1 per cent $AgNO_3$ (w/v) in dH_2O
Developing Buffer (Buffer C)	:	1.5 per cent NaOH, 0.01 per cent $NaBH_4$, 0.015 per cent formaldehyde in dH_2O
Stop Buffer (Buffer D)	:	0.75 per cent $NaCO_3$ in dH_2O
Storage buffer (Buffer E)	:	5 per cent Glycerol in dH_2O

3.5. Fine Chemicals

3.5.1. Enzymes

Taq DNA polymerase enzyme for PCR was provided by Roche (Germany). Super Therm Polymerase (JMR-801) (MEDEK, Turkey) and QIAGEN Taq DNA polymerase with Q-solution (Germany) were also used.

3.5.2. Microsatellite Markers

The genome scan for PEMD family was performed by NHLBI Mammalian Genotyping Service (Contract Number HV48141) as a service grant. A total of 400 microsatellite markers with an average spacing of 8 cM were used (Weber and Broman, 2001).

The genome scan for INAD Family 1, Family 2 and Family 3 had been previously performed in our laboratory but later a tighter scan was performed by NHLBI Mammalian Genotyping Service (Contract Number HV48141) as a service grant. A total of 400 microsatellite markers with an average spacing of 8 cM were used (Weber and Broman, 2001).

Additional polymorphic microsatellite markers for fine mapping of the loci of interest were purchased from Research Genetics (USA), Iontek (Turkey), and Massachusetts General Hospital (MGH, USA).

Additional primers were designed to analyze the candidate loci. The software Tandem Repeats Finder Version 3.21, which was available at the web site http://tandem.bu.edu/trf.html, was used to determine the regions with repeated sequences. Primer pairs were designed using the software PRIMER3, which was available at web site http://workbench.sdsc.edu. The sequences of the designed primers are given in tables 3.1 - 3.8. Resgen markers were purchased at a concentration of 20µM, while markers purchased from Iontek and MGH needed to be diluted to 10µM.

Table 3.1. The sequences of the primers designed to fine map PEMD candidate locus at 3p25.2-p24.3

	Primer Name	**Primer Sequence (5'→3')**
1	D3S17.32-F	CAGAATCACCCACAAGGGAC
	D3S17.32-R	CTGGAACAGTGGTTTCTGCC
2	D3S20.67-F	CCTTCACCTTCCCTTCCTTC
	D3S20.67-R	CCAGAGTAATAATGGAAGAAATTTTG

Table 3.2. The sequences of the primers designed to fine map PEMD candidate locus 16pter

	Primer Name	Primer Sequence (5'→3')
1	D16S0.73Mb-F	AGAATGGTGTGAACCTGGGA
	D16S0.73Mb-R	AGATGGTGGATCCTGTCTGC
2	D16S1.22Mb-F	GGCCCCTGTATGTCTTTTCA
	D16S1.22Mb-R	GAGGCTGAGGCAGGAGAAT
3	D16S1.24Mb-F	GTGAGCCGAGATCACACCA
	D16S1.24Mb-R	TTTTTCCGACTAGCTTCTTTCA
4	D16S1.38Mb-F	ACACACACACACACACACACAA
	D16S1.38Mb-R	GGAGACAGAGCGAGATCCTG
5	D16S1-59Mb-F	CTGAGCCCTAAGTCTGGCAC
	D16S1-59Mb-R	TCCTTCAGGTGAAAGTGGCT
6	D16S2.51Mb-F	AAGTTCTTGGATGTGACGGG
	D16S2.51Mb-R	CCAGCCGAGAGCTGAGAC
7	D16S2.68Mb-F	GGGGGGCAGGAGAAATGCTT
	D16S2.68Mb-R	CGGTCTTCATTTCATGTT
8	D16S3.01Mb-F	ATGGATTGGTCGTGTGTCTG
	D16S3.01Mb-R	AAGTTGCAGTGAGCCGAGAT
9	D16S3.26Mb-F	TAAAACCCAAGGGGAAAAGG
	D16S3.26Mb-R	CTGGGAAACAAGAGCGACAT
10	D16S3.34Mb-F	TTCCCTTCCTCTCTTTCTTCC
	D16S3.34Mb-R	CAGGAGCTCGAGGCTACAGT
11	D16S3.46Mb-F	CTGGACCTCCCAAAGTGCTA
	D16S3.46Mb-R	TGAACCCAAGAAGCAGAGGT
12	D16S6-11Mb-F	GACAGTGGGG AACAGTCCTC
	D16S6-11Mb-R	GCAAAGAAAAGGATTAGGGAA
13	D16S6-20-F	CACTGGGTCTTGTAATTGTGCT
	D16S6-20-R	AGACCATGCCACTTCACTCC
14	D16S5-21Mb-F	AGTGGTGAAGCTGGGAATTG
	D16S5-21Mb-R	GGCTGAATGACAGCATGAGA
15	D16S6-23Mb-F	TGCTTGTTAGGCATTTACGTTC
	D16S6-23Mb-R	GGTGCCTTCTGGCAAATTAC
16	D16S6-42Mb-F	TGGTCATTTACAGAGTTATTGTGATG
	D16S6-42Mb-R	GGCACTACAGCCTTGGTGAT
17	D16S6-51Mb-F	GTCCATCCATCCATCCATCT
	D16S6-51Mb-R	TTGCTAGCTCCAGGGAAGAA
18	D16S6-55Mb-F	CTGTGTAAGCAACTGCAGGC
	D16S6-55Mb-R	CTCTCTGCCCAAGGAAACAG
19	D16S6-57Mb-F	CCACACTTTCACTATTTGGAGC
	D16S6-57Mb-R	CAGGAGGCAGAGGTTGGAGT
20	D16S6-63Mb-F	GTGATCATGCCACTGCACTC
	D16S6-63Mb-R	GGGTCACAAGTATTTGCCCA
21	D16S6-65Mb-F	ATGCATCTTGGTGGGAAAAA
	D16S6-65Mb-R	TGGGAAAACTCATCAGAAACAA
22	D16S6-66Mb-F	GAAGGGAAGTCAACATAGGGG
	D16S6-66Mb-R	CCCCGTAACTACAACACTCACC

Table 3.3. The sequences of the primers designed to fine map INAD candidate locus at 6q25.2-q26

	Primer Name	Primer Sequence (5'→3')
1	D6S162.13Mb-F	TGGTTTCCCCCATACTGTTC
	D6S162.13Mb-R	GCAGGAGAATCACTTGAGCC
2	D6S162-15Mb-F	CAGAGGTTGCAGTTTGCTGA
	D6S162-15Mb-R	GATGTGTGTGTGTGTGTGTGTG
3	D6S162.16Mb-F	CCCCCAAATTCATACATTGA
	D6S162.16Mb-R	AATCACTTGCACCTGGGAAG
4	D6S162.20Mb-F	CTGGAAGCGTTCTTCTGGAT
	D6S162.20Mb-R	GATGAAAGCACAAACAGGGAG
5	D6S162.26Mb-F	TGTCAACTATTAGCAATCATGGG
	D6S162.26Mb-R	AGCTACTCGGGAGGCTGAG
6	D6S162.30Mb-F	TCAAGATCAAGCCACTGCAC
	D6S162.30Mb-R	ATTGACGGTTCCGAGCTAAA
7	D6S162.34Mb-F	TGAAAATAAATACGGTTCTTTACCAA
	D6S162.34Mb-R	TCACCATCAATACTCTGAAATGC
8	D6S162.43Mb-F	ATACACAAAATTGGCCTCGC
	D6S162.43Mb-R	CCATAAGGGTTGTTTTCAGCA
9	D6S163-67Mb-F	CCTGCCACACTGGGACAC
	D6S163-67Mb-R	CCAAGATCACACCACTGCAT
10	D6S163-74-F	AGGTTGCAGTGAGCCGAG
	D6S163-74-R	TCGCCACTCTTACCAAGCTC

Table 3.4. The sequences of the primer pair designed to fine map INAD candidate locus at 6q16.1

	Primer Name	Primer Sequence (5'→3')
1	D6S93-81Mb-F	TCATCATCTCAAACATTATCACTGG
	D6S93-81Mb-R	TGTACTCTAGCCTGGGCGAC

Table 3.5. The sequences of the primers designed to amplify the SNPs within *PARK2*

SNPs GROUP	Primer Name	Primer Sequence (5'→3')
1	D6SNP-G1-F	TTTCTGCATGTCCTCTTCGG
	D6SNP-G1-R	CCGTGAGACTAGATGGCAAAG
2	D6SNP-G2-F	CAGGCCAATTTTACATAAGGC
	D6SNP-G2-R	CAGAAAGCATATATCAGCGCC
3	D6SNP-G3-F	AAAGCACTAAGGCACAGCGT
	D6SNP-G3-R	TTGACCACAAATCCAAAGCA

Table 3.6 The sequences of the primers designed to fine map INAD candidate locus at 11p13-q12.1

Region	Primer Name	Primer Sequence (5'→3')
1	D11S42.63Mb-F	ATTGATGGATGGATGGATGG
	D11S42.63Mb-R	TTGCTTACAATCTGGAGCATTT
2	D11S42.79Mb-F	TTCACACAGGCATGAAAATC
	D11S42.79Mb-R	TGATGGTGGAAAGAAACATCA
3	D11S43.17Mb-F	ATGTTGTGCCCATGTACCCT
	D11S43.17Mb-R	TTCTTTTATCTTCTTTATTTTTGGCTT
4	D11S46.42Mb-F	TTGAGTCTGGAAGGTGGAGG
	D11S46.42Mb-R	TTTTAAAGGCCATTTATTATGCAC
5	D11S47.70Mb-F	GGCGGATCTTGCAGTGAG
	D11S47.70Mb-R	TTTTGAATTACATAGGATAGGGAGG

Table 3.7 Sequences of primer pair designed to fine map INAD candidate locus at 14q32.13-q32.33

Region	Primer Name	Primer Sequence (5'→3')
1	D14S100.72Mb-F	CGCTGTGAGGAGCTGTAAGA
	D14S100.72Mb-R	ATCCATCCACTCACCCATTC

Table 3.8 Sequences of primer pair designed to fine map INAD candidate locus at16p13.2

Region	Primer Name	Primer Sequence (5'→3')
1	D16S7.53Mb-F	ATTGAGAGTCTGCACCATGC
	D16S7.53Mb-R	CACTCCAGCCTGACAACAGA

3.5.3 Other Fine Chemicals

Deoxyribonucloside triphosphates (dNTPs) were purchased from Roche (USA). PCR products to be sequenced were purified by using the QIAquick PCR Purification Kit (Qiagen, Germany).

3.6. Equipment

Autoclave	:	Model MAC-601 (Eyela, Japan) Prior-Clave (UK)
Balance	:	Electronic Balance (GecAvery, UK) BJ210C Precisa (Switzerland) BJ2100D Precisa (Switzerland)
Centrifuges	:	Centrifuge (DuPont Instruments, USA) 5415C (Eppendorf, Germany) Mini Spin Plus Eppendorf (Germany)
Deep Freezers	:	-20^{o}C (Bosch, Germany) -20^{o}C (AEG, Turkey) -70^{o}C (GFL, Germany)
Documentation System	:	Gel Doc 2000 Bio-Rad (USA)
Electrophoretic Equipment	:	Wide Mini Sub Cell Gt Bio-Rad (USA) Sequi-Gen Sequencing Cell Bio-Rad (USA)
Incubators	:	Plus Series Gallenkamp (Germany) Orbital Gallenkamp (Germany)
Magnetic Stirrer	:	Hotplate Magnetic Stirrer, HS31 Chiltern (UK) MR 3001 Heidolph (Germany)
Minishaker	:	IB InterMed (Denmark) Rotamax Heidolph (Germany)
Ovens	:	80°C (Heraeus, Germany)

Power Supplies	:	Power Pac Model 3000 Bio-Rad (USA) Fotoforce 250 Fotodyne (USA)
Refrigerator	:	4°C Arçelik (Turkey)
Spectrophotometer	:	Lambda 3 UV/VIS (Perkin-Elmer, USA)
Thermocyclers	:	MJ Research (USA) Bio-Rad Mycycler (USA)
Transilluminators	:	Chromato-Vue Transilluminator, Model 1 TM-20UVP (USA) Fluorescent Table Consort (Belgium)
Vortex	:	REAX top Heidolph (Germany)
Waterbath	:	Water Bath D 3162 Köttermann Labortechnik (Germany)
Water Purification System	:	Millipore Elix 3 Millipore (France)

3.7. Electronic Database Information

The database used for obtaining the physical maps of polymorphic markers and genes in the relevant loci was GeneBank (http://ncbi.nlm.nih.gov). The database used for obtaining the genetic maps was Marshfield Clinics (http://www.marshmed.org/genetics). The database used to search polymorphic markers and determine the chromosomal positions was UCSC Genome Bioinformatics (http://genome.ucsc.edu/index.html).

The database used for obtaining information about the disorders was Online Mendelian Inheritance in Man (http://www.ncbi.nlm.nih.gov/Omim).

The database used for repeat search in the genome was Tandem Repeats Finder (http://tandem.bu.edu/trf/trf.html). The database used for designing primer pairs was The Biology WorkBench (http://workbench.sdsc.edu), which provides the PRIMER3 software. The program used for searching a pair of PCR primers against the human genome sequence database was In-Silico PCR provided by UCSC. The UCSC Genome Browser database was used to determine the chromosomal positions of the markers, and UCSC Table Browser database was used to search polymorphic markers (http://genome.ucsc.edu).

The database used for obtaining the software for linkage analyses and pedigree drawings was the Laboratory of Statistical Genetics at Rockefeller University (http://linkage.rockefeller.edu). Program provided by Progeny software of Progeny LAB 6 was also used for pedigree drawing (http://www.progeny2000.com).

4. METHODS

4.1. DNA Extraction from Peripheral Blood Samples

Genomic DNA from patients and their family members were isolated from 10 ml of peripheral blood samples that had been collected into sterile vacutainer tubes containing K_2EDTA as anticoagulant. The blood sample was transferred into a 50 ml falcon tube, and 30 ml of cold cell lysis buffer was added for every 10 ml sample. After mixing thoroughly, the mixture was kept for 15 minutes (min) at 4°C to allow the disintegration of plasma membranes. The samples were centrifuged at 5000 revolutions per minute (rpm) and 4°C for 10 min to collect leukocyte nuclei. The supernatant containing cell debris was discarded, and the pellet of leukocyte nuclei was washed by suspending in ten ml of cell lysis buffer and centrifugation for 10 min. The supernatant was discarded, and the nuclei were resuspended in five ml of nuclei lysis buffer by vortexing. After the entire pellet had been dissolved, 80 µl of 10 per cent SDS and 50 µl of Proteinase K (20 mg/ml) were added and mixed gently by rolling and rocking the tube by hand. When the solution became jelly-like, the sample was incubated either at 37°C overnight or at 56°C for three hours (hr) to digest the nuclear proteins. For blood samples that had a lot of coagulation, the sample was incubated at 56°C overnight. In order to get rid of the protein residues, 1.7 ml of 9.5 M NH_4Ac was added, and the sample was shaken vigorously to salt out the proteins. The sample was then centrifuged at 5000 rpm at room temperature for 25 min. The supernatant was transferred into a clean 50 ml Falcon tube. Two volumes of ethanol were added to precipitate out DNA. After DNA threads become visible and collected at the surface, DNA was fished out carefully with a micropipette tip and transferred into a 1.5 ml Eppendorf tube. Residual ethanol was air-dried. Depending in its estimated quantity, DNA was dissolved in 200-1000 µl of TE buffer and stored at -20°C.

4.2. Linkage Analysis

4.2.1. PCR

PCR for a Resgen marker was carried out in a total volume of 11 µl, consisting of 1 X PCR buffer, 0.3 µl of each primer pair, 0.2 mM of dNTP, 125 ng of genomic DNA, 0.15 U Taq DNA polymerase and sufficient dH_2O to adjust the volume. The PCR conditions were as follows: an initial denaturation step at 95°C for two min, followed by 30 cycles of denaturation at 94°C for 45 sec, annealing at the appropriate temperature and elongation at 72°C, and a final extension step for 10 min at 72°C. The times of annealing and elongation were determined subsequent to optimization.

PCR for markers purchased from Iontek or MGH was carried out in a total volume of 25 µl, consisting of 1 X PCR buffer, 1 µl of each primer pair, 0.2 mM of dNTP, 125 ng of genomic DNA, 0.15 U Taq DNA polymerase and sufficient dH_2O to adjust the volume. The PCR conditions were as follows: an initial denaturation step at 95°C for two min, followed by 30 cycles of denaturation at 94°C for 45 sec, annealing at the appropriate temperature and elongation at 72°C, and a final extension step for 10 min at 72°C. The times of annealing and elongation were determined subsequent to optimization.

Touchdown PCR conditions were also applied whenever needed. The PCR conditions were as follows: an initial denaturation step at 95°C for three min, followed by 20 cycles of denaturation at 94°C for 30 sec, annealing at the appropriate temperature for 45 sec and elongation at 72°C for 1 min. During this period, the temperature was decreased by 0.5°C for each cycle. The conditions of the second part of touch-down PCR were as follows: 30 cycles of denaturation at 84°C for 30 sec, annealing at the last temperature reached after the first part of touchdown PCR for 45 sec and elongation at 72°C for one min.

PCR products were mixed with 10 X Sample buffer in a 1:1 ratio. The samples were loaded onto an eight or 12 per cent denaturing polyacrylamide gel after incubating at 95°C for five minutes, as described in sections 4.3.3 and 4.3.4. Alleles were resolved under a

constant power appropriate for the electrophoresis type and visualized by silver staining as described in Section 4.3.8.

Fine mapping was applied whenever a candidate region was identified after examining the genome scan results. The deduced annealing temperatures, average or range of the product sizes and repeat types of the markers are given in tables 4.1 to 4.21. In each table, "a" stands for GenBank Sequence map, "b" for Marshfield Genetic Map, "c" for non-informative markers, "d" for primers designed in our laboratory, "f" for markers used in our laboratory for fine mapping, "g" for primers that could not be optimized and "m" for markers used by NHLBI Mammalian Genotyping Service for genome-scan. In all PCR reactions, 10X PCR buffer was used and there were no additives unless stated otherwise.

Table 4.1. Properties of 45 markers used for fine mapping at 16pter-p13.13 for PEMD

Marker Name	Mb[a]	cM[b]	Product Size (bp)	Repeat Type	Annealing Temperature (°C)	Status
TTTA028	0.60	2.3	179	TETRA	-	m
D16S0.73 [d, c]	0.73	-	198	TETRA	61-51 touchdown	f
D16S525 [g]	0.98	-	143-175	DI	-	f
D16S1.22 [d, c]	1.22	-	193	TETRA	58-48 touchdown	f
D16S1.24 [d, c]	1.24	-	183	TETRA	55.4	f
D16S1.38 [d, g]	1.38	-	186	DI	-	f
D16S1.59 [d]	1.59	-	197	DI	54.2	f
D16S3024	1.59	7.05	208-248	DI	53.1	f
D16S3395	1.94	6.08	124-137	TRI	55	f
D16S3124	2.39	7.05	93-103	DI	53.1	f
D16S2.51 [d, g]	2.51	-	186	TETRA	-	f
D16S2.68 [d]	2.68	-	197	TETRA	55.4	f
D16S3.01 [d, c]	3.01	-	147	TETRA	55.4	f
D16S3070 [c]	3.03	7.61	153-173	DI	57	f
D16S2618	3.19	-	135	TRI	54.5	f
D16S3.26 [d]	3.26	-	188	DI	53	f
D16S3.34 [d, g]	3.34	-	199	TETRA	-	f
D16S475	3.41	160-189	183	TETRA	54.6	f
D16S3.46 [d, g]	3.46	-	186	TRI	-	f
D16S2622 [c]	3.64	8.16	83	TETRA	53.1	f
D16S3065 [g]	3.76	8.16	152-162	DI	-	f
D16S3084	4.21	8.71	83-101	DI	58-48 touchdown, 5M Betaine	f
D16S3072 [c, g]	4.27	8.71	148-168	DI	55.8	f
D16S3134 [g]	5.16	7.61	161-174	DI	-	f
D16S5.21 [d]	5.21	-	197	TETRA	55.8	f
D16S510 [c]	5.68	10.36	217-287	DI	54.8	f
D16S6.11 [d]	6.11	-	192	DI	52.1	f

Table 4.1. Properties of 45 markers used for fine mapping at 16pter-p13.13 for PEMD (continued)

D16S6.20 [d]	6.20	-	195	TETRA	52.5	f
D16S2616	6.21	11.46	121-139	TRI	-	m
D16S6.23 [d]	6.23	-	196	DI	57.6	f
D16S3392	6.30	11.46	138-170	TETRA	53	f
D16S6.42 [d]	6.42	-	197	TETRA	57.6	f
D16S6.51 [d]	6.51	-	181	TETRA	57	f
D16S6.55 [d]	6.55	-	134	TETRA	56.2	f
D16S6.57 [d]	6.57	-	200	TRI	58	f
D16S6.63 [c, d]	6.63	-	162	TETRA	58	f
D16S6.65 [d]	6.65	-	187	DI	55.9	f
D16S6.66 [d]	6.66	-	198	DI	58	f
D16S3128	6.98	12.57	140-174	DI	60.3	f
D16S3088	7.15	13.12	203-223	DI	51.5	f
D16S3092	7.50	13.67	196-212	DI	56.4	f
D16S768	8.31	-	158	TETRA	54.5	f
D16S3020 [g]	8.77	16.97	56-94	DI	-	f
D16S748	12.05	22.65	187-214	TRI	55	m&f

Table 4.2. Properties of seven markers used for fine mapping at 3p25.2-p24.3 for PEMD

Marker Name	Mb[a]	cM[b]	Product Size (bp)	Repeat Type	Annealing Temperature (°C)	Status
D3S2403	13.14	37.20	248-292	TETRA	-	m
D3S2338 [g]	16.82	42.1	179-197	DI	55	f
D3S17-92 [d]	17.92	-	198	TETRA	53.5	f
D3S3510 [c]	19.07	42.1	279-289	DI	53.5	f
D3S3726	19.50	42.64	185-207	DI	49.3	f
D3S20-67 [d, g]	20.67	-	190	DI	-	f
D3S3038	21.92	44.81	198	TETRA	-	m

Table 4.3. Properties of three markers used for confirmation and fine mapping at 6q14.1-q16.1 for PEMD

Marker Name	Mb[a]	cM[b]	Product Size (bp)	Repeat Type	Annealing Temperature (°C)	Status
D6S1031	77.51	88.63	260	TRI	-	m
D6S1627	85.46	92.85	98-114	DI	56.5	f
D6S1056	94.15	103	250	TETRA	-	m

Table 4.4. Properties of five markers used for fine mapping at 6p23-p22.2 for PEMD

Marker Name	Mb[a]	cM[b]	Product Size (bp)	Repeat Type	Annealing Temperature (°C)	Status
D6S2434	14.05	25.1	222	TRI	-	m
D6S429	14.81	26.71	222-238	DI	54.8	f
D6S1959	-	34.23	197	TETRA	-	m
D6S109	20.11	34.23	169-193	DI	56	f
D6S2439	-	42.27	154	TETRA	-	m

Table 4.5. Properties of three markers used for confirmation and fine mapping at 6p21.31-p21.1 for PEMD

Marker Name	Mb[a]	cM[b]	Product Size (bp)	Repeat Type	Status
D6S1051	37.03	50.75	225	TETRA	m
D6S1602[g]	37.82	50.75	194-208	DI	f
D6S1017	41.78	63.28	151-171	DI	m

Table 4.6. Properties of three markers used for confirmation and fine mapping at 6p12.3-q12 for PEMD

Marker Name	Mb[a]	cM[b]	Product Size (bp)	Repeat Type	Annealing Temperature (°C)	Status
D6S2410	50.75	73.13	158	TETRA	-	m
D6S1695	62.42	80.99	155-163	DI	51.5	f
D6S1053	64.64	80.45	312	TETRA	-	m

Table 4.7. Properties of three markers used for confirmation and fine mapping at 18q12.3-q21.1 for PEMD

Marker Name	Mb[a]	cM[b]	Product Size (bp)	Repeat Type	Annealing Temperature (°C)	Status
D18S535	36.40	64.48	150	TETRA	-	m
D18S865	36.59	64.48	197	TETRA	55	f
D18S851	48.36	-	256-276	TETRA	-	m

Table 4.8. Properties of three markers at *PANK2* locus (20p13) used for confirmation and fine mapping for all INAD families

Marker Name	Mb[a]	cM[b]	Product Size (bp)	Repeat Type	Annealing Temperature (°C)	Status
AAAT007	-	2.6	-	-	-	m
D20S889	3.9	11.20	262-296	DI	56	f
D20S482	4.45	12	153	TETRA	-	m

Table 4.9. Properties of 23 markers used for fine mapping at 6q25.2-q26 for INAD Family 1

Marker Name	Mb[a]	cM[b]	Product Size (bp)	Repeat Type	Annealing Temperature (°C)	Additives	Status
D6S2436	154.23	154.64	200	TETRA	-	-	m
D6S437	158.73	161.59	129-163	DI	51	-	f
D6S969	159.25	161.55	110	TETRA	54.8	2.5 mM Mg	f
D6S1035	160	164.78	131	TRI	-	-	m
D6S1581	160.24	164.78	215-229	DI	55	-	f
D6S1579	160.99	166.39	147-163	DI	57	2.5 mM Mg	f
D6S1550[c]	161.88	166.39	122-136	DI	54.8	-	f
D6S411	161.95	166.39	151-159	DI	56.6	Q sln, 1.24% formamide	f
D6S162.13[d]	162.13	-	198	TETRA	56.6	-	f
D6S162.15[d,g]	162.15	-	155	DI	-	-	f
D6S305	162.16	166.39	204-230	DI	57	-	f
D6S162.16[d]	162.16	-	191	TETRA	53.5	-	f
D6S162.20[c,d]	162.20	-	169	DI	53.5	-	f
D6S162.26[d,g]	162.26	-	187	TETRA	-	-	f
D6S162.30[d]	162.30	-	191	TRI	51.4	-	f
D6S162.34[d]	162.34	-	183	DI	57.5	-	f
D6S162.43[d]	162.43	-	195	DI	57.5	-	f
D6S955	162.51	167.78	153	TETRA	58.4	-	f
D6S1008	163.59	-	246	TETRA	55	-	f
D6S163-67[c,d]	163.67	-	199	TETRA	56.2	Q sln, 2% DMSO	f
D6S163.74[d,g]	163.74	-	200	TETRA	-	-	f
D6S1277	164.26	173.31	292	TETRA	-	-	m
D6S1027	168.95	187.23	117-138	TRI	-	-	m

Table 4.10. Properties of three markers amplifying regions containing SNPs at *PARK2* region in INAD Family 1

Marker	Amplified region	SNP#	Product Size (bp)	Annealing Temperature	Additives
D6SNP-G1[d]	162180200-162180999	6	732	54.1	2% DMSO
D6SNP-G2[d,g]	162247200-162247999	X	654	-	-
D6SNP-G3[d]	162247200-162247999	4	796	54.1	2% DMSO

Table 4.11. Properties of 19 markers used for fine mapping at 11p for INAD Family 1

Marker Name	Mb[a]	cM[b]	Product Size (bp)	Repeat Type	Annealing Temperature (°C)	Additives	Status
D11S1392	34.59	43.16	200-220	TETRA	-	-	m
D11S1279	40.46	50.88	177	TETRA	56.2	Roche	f
D11S905	40.93	51.95	208-228	DI	54.2	2.48% glycerol	f
D11S4180	41.48	53.02	200-210	DI	58.8	-	f
D11S1779	41.83	53.02	275-287	DI	55.5	Q sln, 2% DMSO	f
D11S1785	42.34	53.87	268-276	DI	55	-	f
D11S42.63 [c, d]	42.63	-	200	TETRA	57.5	-	f
D11S42.79 [c, d]	42.79	-	199	TRI	57.5	-	f
D11S1763	42.82	53.56	182-190	DI	55	-	f
D11S43.17 [d]	43.17	-	151	TETRA	57.5	-	f
D11S1993	43.56	54.09	228	TRI	-	-	m
D11S1393	43.95	54.75	198-210	TETRA	55.8	1.24% formamide	f
D11S1915	45.54	57.83	285	TETRA	57.2	-	f
D11S46.42 [d]	46.42	-	193	TETRA	53.8	-	f
D11S4109 [g]	47.59	58.40	155-185	DI	-	-	f
D11S47.70 [d, g]	47.70	-	189	TETRA	-	-	f
D11S1978	48.54	58.40	250-298	TETRA	56.2	2.48% glycerol	f
D11S2363	58.99	58.40	272	TETRA	-	-	m

Table 4.12. Properties of seven markers used for fine mapping at 14q for INAD Family 1

Marker Name	Mb[a]	cM[b]	Product Size (bp)	Repeat Type	Annealing Temperature (°C)	Status
D14S617	91.27	105.53	141	TETRA	-	m
D14S1434	-	113.17	208-232	TETRA	-	m
ATGG002	-	119	-	-	-	m
D14S305 [c]	100.1	-	233	TETRA	54.5	f
G09851	100.43	-	145	TRI	55	f
D14S100.72 [d]	100.72	-	189	TETRA	53.5	f
D14S543	103.65	125.88	255-315	TETRA	52.3	f
ATT198Z	-	134.5	-	-	-	m

Table 4.13. Properties of six markers used for fine mapping at 7q36 for INAD Family 1

Marker Name	Mb[a]	cM[b]	Product Size (bp)	Repeat Type	Annealing Temperature (°C)	Status
GATA104	-	155	-	TETRA	-	m
D7S3070	150.52	163.03	190	TETRA	-	m
D7S1815	151.83	166.48	185	TETRA	55	f
GATA2C08	152.43	-	267-268	TETRA	54.5	f
D7S1823	153.42	173.71	230	TETRA	55	m
D7S550	155.01	178.41	177-200	DI	53	f
MFD442-GTTT002	155.41	178.6	-	-	-	m

Table 4.14. Properties of five markers used for fine mapping at 8p23 for INAD Family 1

Marker Name	Mb[a]	cM[b]	Product Size (bp)	Repeat Type	Annealing Temperature (°C)	Status
ATT023	4.13	4.3	-	-	-	m
D8S1798	5.08	6.65	145-165	DI	53.1	f
TTCA004P	9.16	16	-	-	-	m
D8S11086	9.18	-	188	DI	55	f
ATT070	14.96	30	-	-	-	m
D8S136 [g]	22.49	43.96	71-89	DI	-	f
ATAA018P	-	43.4	-	-	-	m

Table 4.15. Properties of six markers used for fine mapping at 7q22 for INAD Family 1

Marker Name	Mb[a]	cM[b]	Product Size (bp)	Repeat Type	Status
D7S2477	0.26	0	142-170	DI	m
D7S1484 [g]	0.39	-	399	TETRA	f
D7S2474 [g]	0.95	3.13	135-151	DI	f
D7S1819	4.46	7.44	179	TETRA	m

Table 4.16. Properties of three markers used for fine mapping at 6q16 for INAD Family 1

Marker Name	Mb[a]	cM[b]	Product Size (bp)	Repeat Type	Annealing Temperature (°C)	Additives	Status
D6S1274	93.46	101.55	371	TETRA	-	-	p
D6S93.81 [d, c]	93.81	-	153	TETRA	58.4	Q sln	f
D6S1056	94.15	102.81	250	TETRA	-	-	p

Table 4.17. Properties of three markers used for fine mapping at 16p for INAD Family 1

Marker Name	Mb[a]	cM[b]	Product Size (bp)	Repeat Type	Status
D16S3092	7.50	13.67	196-212	DI	p
D16S7.53 [d, g]	7.53	-	138	DI	f
D16S418	7.58	14.77	166-188	DI	p

Table 4.18. Properties of seven markers used for fine mapping at 2q37 for INAD Family 2

Marker Name	Mb[a]	cM[b]	Product Size (bp)	Repeat Type	Annealing Temperature (°C)	Status
D2S1363	226.74	227	177	TETRA	-	m
D2S427	232.03	236.7	244-254	TETRA	-	m
D2S2348	233.93	242.17	171-199	DI	55.2	f
GATA23A02	-	248	-	TETRA	-	m
D2S338	237.01	250.54	273-291	DI	51	f
D2S2968	237.86	251.94	180	TETRA	-	m
D2S237-95[c]	237.95	-	186	TETRA	59.4	f
AGAT021	-	266.2	-	-	-	m

Table 4.19. Properties of seven markers used for fine mapping at 21q22.13-q22.3 for INAD Family 2

Marker Name	Mb[a]	cM[b]	Product Size (bp)	Repeat Type	Annealing Temperature (°C)	Status
D21S2052	27.74	-	120	TETRA	-	m
D21S1440	38.06	36.77	162	TRI	-	m
D21S1809	38.81	-	208	TETRA	52.1	f
D21S2055	40.11	40.49	117-193	TETRA	-	m
D21S231[c]	40.83	45.55	180-190	DI	56.6	f
D21S1235	41.38	-	112-144	TRI	53.8	f
D21S1411	43.03	51.49	239	TETRA	-	m
D21S1446	43.03	57.77	221	TETRA	-	m

Table 4.20. Properties of four markers used for fine mapping at 18q12.3-q21.1 for INAD Family 2

Marker Name	Mb[a]	cM[b]	Product Size (bp)	Repeat Type	Annealing Temperature (°C)	Additives	Status
G10491	35.73	-	190	TETRA	58.4	Q sln	f
D18S535	36.40	64.48	150	TETRA	-	-	m
D18S865	36.59	64.48	197	TETRA	55	-	f
D18S851	48.36	-	256-276	TETRA	-	-	m

Table 4.21. Properties of three markers used for fine mapping at 8p21.2-p12 for INAD Family 3

Marker Name	Mb[a]	cM[b]	Product Size (bp)	Repeat Type	Annealing Temperature (°C)	Additives	Status
TTA024	-	49.9	-	-	-	-	m
D8S1048	26.87	54.28	206	TETRA	-	-	m
D8S1809	28.24	54.98	154-174	DI	53.1	2.48% glycerol	f
D8S1477	32.18	60.34	145	TETRA	-	-	m
D8S1110	53.34	67.27	262-286	TETRA	-	-	m

4.2.2. Analysis of PCR Products

To estimate the amount of amplification, a five µl aliquot of PCR product was mixed with five µl of 1 X loading buffer, loaded on a two per cent agarose gel containing 15 µg Ethidium Bromide and electrophoresed in 0.5 X TBE at 150 volts for 10 minutes. The bands were subsequently visualized over a UV light transilluminator. To confirm the sizes of the PCR products, to detect any unspecific amplification and DNA size variation, and to resolve the alleles, the products were run on an eight per cent denaturing gel as described in Section 4.3.3 and visualized by silver staining as described in Section 4.3.5.

4.2.3. Preparation of Denaturing Polyacrylamide Gels

Two different sizes of electrophoresis gels were used. The smaller denaturing polyacrylamide gel was cast in a 21 x 40 cm sequencing apparatus that was assembled using 0.4 mm spacers. Thirty-five ml of eight or 12 per cent Instagel was mixed with 300 µl of 10 per cent APS and 30 µl of TEMED and immediately poured between the glass plates of the apparatus. A sharks-tooth comb was inserted in an inverted position. The gel was allowed to polymerize for at least forty-five minutes before electrophoresis. The larger denaturing polyacrylamide gel was cast in a 38 x 30 cm sequencing apparatus that was assembled using 0.4 mm spacers. 45 ml of eight or 12 per cent Instagel was mixed with 350 µl of 10 per cent APS and 35 µl of TEMED and poured between the glass plates of the apparatus. For samples with short lengths of 50 to 100 bp, 12 per cent Instagel was used to impede diffusion.

4.2.4. Denaturing Polyacrylamide Gel Electrophoresis

Electrophoresis was carried out in 1 X TBE buffer heated for six minutes in a microwave oven to raise its temperature to 55-60°C. For small electrophoresis apparatus, the gel was initially prerun in the hot buffer for 15 min at a constant power of 45 W in order to allow the gel temperature to rise to 40-45°C, whereas for the larger one, the prerun was performed at a constant power of 70 W to allow the gel temperature to rise to 50-55°C. The DNA samples were mixed in 1:1 ratio with 10 X Sample buffer, denatured at 95°C in a heat block for five min, and immediately chilled on ice. The comb was reoriented in the correct position to form wells, and the upper part of the gel was cleaned from urea and gel particles by squirting electrophoresis buffer. Depending on their band intensities on agarose gels, four to six µl of each sample was loaded into individual slots. The gel was run at a constant power of 35 W for the small electrophoresis apparatus and at a constant power of 65 W for the large one. The duration of the electrophoresis was adjusted according to allele sizes and the predicted distances between the alleles. After electrophoresis, the gel was silver stained to visualize the alleles as explained in Section 4.3.5.

4.2.5. Silver Staining

When electrophoresis was complete, the glass plates were separated. The gel usually remained attached to one of them and was removed with the help of filter paper. It was transferred to Buffer B. The polyacrylamide gel run in the smaller electrophoresis apparatus was shaken for eight min, whereas the gel run in the larger one was shaken for twelve min. The gel was washed twice with dH_2O to remove excess silver. The gel was then incubated in Buffer C until bands appeared. Lastly, the gel was transferred to Buffer D for ten minutes to stop the reaction. Paper towels were used to prevent tearing and folding of the gel while discarding the buffers after each step. Whenever bands were weakly stained and difficult to read, staining was repeated. It was very important to finally wash the gel well, at least five times with dH_2O, to prevent darkening of the gel later. The gel was sealed in a transparent folder containing glycerol for storage and documentation (Kavaslar *et al.*, 2000).

4.3. Computerized Linkage Programs

Linkage analysis was performed under the assumption of autosomal recessive inheritance, full penetrance, a disease gene frequency of 1 in 100,000, equal recombination frequencies for males and females, and equal frequencies of marker alleles. Two-point lod scores were calculated using the MLINK program of the FASTLINK 4.1 package (Ott, 1991). Maximum lod scores and MLEs of recombination fractions were determined using the ILINK program of the same package. SimWalk2 version 2.0 beta was used for multipoint parametric linkage analysis and construction of the haplotypes, allowing minimum number of recombination events. (Sobel *et al.*, 1996)

Mapviewer tool of NCBI database (National Center for Biotechnology Information, http://www.ncbi.nih.gov/Mapviwer) was used to explore the genes within the identified homozygous blocks. The functions of those genes were then investigated using databases to determine the candidate genes responsible for the diseases.

4.4. DNA Sequence Analysis

The samples to be analyzed with SNPs were subjected to sequence analysis, which was performed on purified PCR products.

A DNA fragment to be sequenced was amplified in a 75µl reaction volume and purified from the unused primers, dNTPs, and genomic DNA by a QIAquick-spin column provided by QIAGEN kit. The purification was performed by applying the QIAGEN protocol. The purity of the eluted template was checked on a two per cent agarose gel and then was ascertained on an eight per cent denaturing polyacrylamide gel.

Purified DNA templates were sent to Iontek (Turkey) for sequence analysis.

5. RESULTS

Within the framework of linkage studies, homozygosity mapping was performed for the autosomal recessive disorders PEMD and INAD. The candidate gene loci were further analyzed with additional markers. Computerized lod score analyses were performed to assess the significance of the obtained data, whenever necessary.

5.1. Linkage Analyses in PEMD Family

The genome scan performed by NHLBI Mammalian Genotyping Service revealed several candidate loci that possibly harbored the gene responsible for PEMD. The candidate regions were further fine mapped by using primers for microsatellite markers either reported by Marshfield or those designed in this study. Five candidate loci were assessed as candidate after the first evaluation of the genome-wide scan data. Three of them were on chromosome 6 and others on chromosomes 3 and 18. They were investigated by genotyping with additional microsatellite markers. All were excluded by homozygosity mapping. The haplotypes of the family members for each loci are given in tables 5.1-5.5. In the tables presented throughout the results part, “M” stands for mother, “F” for father, “P” for patient and “*” for markers used by NHLBI Mammalian Genotyping Service for genome scan Figure 5.1 shows the silver-stained gel for alleles of D18S865 in PEMD family.

Table 5.1. Haplotypes of patients and their parents in PEMD family at 3p25.2-p24.3

Individual		**406**	**407**	**415**	**416**	**401**	**501**	**601**	**405**	**502**	**603**	**506**	**505**	**604**
ID		**M**	**F**	**M**	**F**	**M**	**F**	**P**	**M**	**F**	**P**	**M**	**F**	**P**
MARKER	**POSITION (Mb)**													
D3S2403*	13.14	-	6 8	5 8	8 8	-	-	-	8 8	5 8	8 8	8 8	6 6	8 6
D3S17-92	17.92	1 4	1 1	1 3	3 3	3 2	3 2	2 2	4 4	3 1	1 4	3 1	4 3	1 4
D3S3726	19.50	2 3	2 2	3 2	3 2	1 4	2 2	4 2	2 3	3 2	2 2	1 2	2 3	2 2
D3S3038*	21.92	-	6 7	2 1	1 7	-	-	-	7 7	6 7	7 7	4 4	7 6	4 7

Table 5.2. Haplotypes of patients and their parents in PEMD family at 6q14.1-q16.1

Individual		406	407	415	416	401	501	601	405	502	603	506	505	604
ID		M	F	M	F	M	F	P	M	F	P	M	F	P
MARKER	POSITION (Mb)													
D6S1031*	77.51	3 6	1 6	2 6	6 6	-	-	-	3 6	1 6	6 6	6 2	3 6	6 3
D6S1627	85.46	3 5	4 4	3 4	4 5	4 5	1 5	5 5	2 5	-	5 5	4 6	2 4	2 5
D6S1056*	94.15	2 3	6 6	7 3	2 4	-	-	-	2 3	3 3	2 3	7 3	6 2	3 6

Table 5.3. Haplotypes of patients and their parents in PEMD family at 6p23-p22.2

Individual		406	407	415	416	401	501	601	405	502	603	506	505	604
ID		M	F	M	F	M	F	P	M	F	P	M	F	P
MARKER	POSITION (Mb)													
D6S2434*	14.05	3 5	3 3	5 2	2 3	-	-	-	5 3	-	3 3	3 3	4 2	3 4
D6S429	14.81	-	-	-	-	1 2	2 2	1 2	1 2	1 2	1 2	-	1 2	1 2
D6S1959*	20.02	3 2	3 2	2 1	3 3	-	-	-	2 3	1 3	3 3	2 3	2 1	2 2
D6S109	20.11	2 3	2 3	3 3	2 2	3 3	3 3	3 3	2 3	2 3	3 3	1 2	2 3	1 1
D6S2439*	24.41	4 5	8 7	4 2	4 5	-	-	-	4 5	8 5	5 5	4 4	3 6	4 3

Table 5.4. Haplotypes of patients and their parents in PEMD family at 6p12.3-q12

Individual		406	407	415	416	401	501	601	405	502	603	506	505	604
ID		M	F	M	F	M	F	P	M	F	P	M	F	P
MARKER	POSITION (Mb)													
D6S2410*	50.75	2 2	2 2	2 3	2 2	-	-	-	2 2	2 2	2 2	3 2	2 1	2 3
D6S1695	62.42	3 3	2 3	2 3	3 3	1 1	1 2	1 2	-	1 2	2 2	2 2	1 2	1 2
D6S1053*	64.64	2 6	5 1	6 4	5 7	-	-	-	2 6	2 6	6 6	7 5	5 4	5 7

Table 5.5. Haplotypes of patients and their parents in PEMD family at 18q12.3-q21.1

Individual		406	407	415	416	401	501	601	405	502	603	506	505	604
ID		M	F	M	F	M	F	P	M	F	P	M	F	P
MARKER	POSITION (Mb)													
D18S535*	36.40	3 5	3 2	4 5	5 5	-	-	-	3 5	5 4	5 5	7 5	5 5	5 5
D18S865	36.59	3 3	1 4	2 3	2 2	1 3	1 4	1 4	3 3	2 4	3 4	2 3	2 4	3 4
D18S851*	48.36	4 6	4 3	4 4	2 5	-	-	-	6 6	4 5	4 6	3 4	5 2	2 4

After the exclusion of the five candidate loci, the candidate locus at 16pter was considered also a candidate region for harboring the gene responsible for the disease. The genome wide scan results were noninformative at the region, so it did not appear as a strong candidate locus. Genotyping with additional markers confirmed the shared homozygosity in the three affected individuals from whom DNA samples were available. Likely, the two deceased ones also were homozygous, since all their parents carried the haplotype. Such shared haplotype was consistent with descent from a common ancestor, although the blood relation was not known for all parents. This analysis, in addition, narrowed down the locus to a maximum 3.26 Mb region at the 16pter telomeric to D16S3-26. The haplotype data are given in Figure 5.3. Two-point and multi-point lod score analyses were also done to assess the significance of the results. Two-point linkage analysis for 25 markers yielded lod scores higher than 3.00 at a recombination fraction of zero for most of the markers in the region spanning 0 – 6.98 Mb (Table 5.6). Multi-point lod scores were also calculated and found to curve up around six from 16pter to D16S6-66 (Figure 5.4). However, an ancestral crossover event telomeric to D16S3-26 was detected by haplotype analysis in individual 407, and this narrowed down the gene locus to a 3.26 Mb interval at 16pter. The reasoning was as follows: as the presumable consanguinity between individuals 406 and 407 was not presented to the linkage programs and as only the DNA of a single child was available, no linkage information could be obtained from this core family. Therefore, the linkage programs did not take into consideration the haplotype data of the family. This data limits the gene locus to 3.26 Mb down from 6.66 Mb.

The homozygous region between 7.50 Mb-12.05 Mb shared by two PEMD patients contains the *ABAT* (4-Aminobutyrate aminotransferase) gene. Mutations in this gene were found to be associated with 4-Aminobutyrate aminotransferase deficiency disease. Since PEMD shares some clinical characteristics with this disease, a linkage test was applied to exclude that region. The family was genotyped with marker D16S768 at 8.31Mb, and the patients were found to carry different alleles, excluding the region. Figure 5.2 shows the silver-stained gel for the alleles of D16S768 in PEMD family.

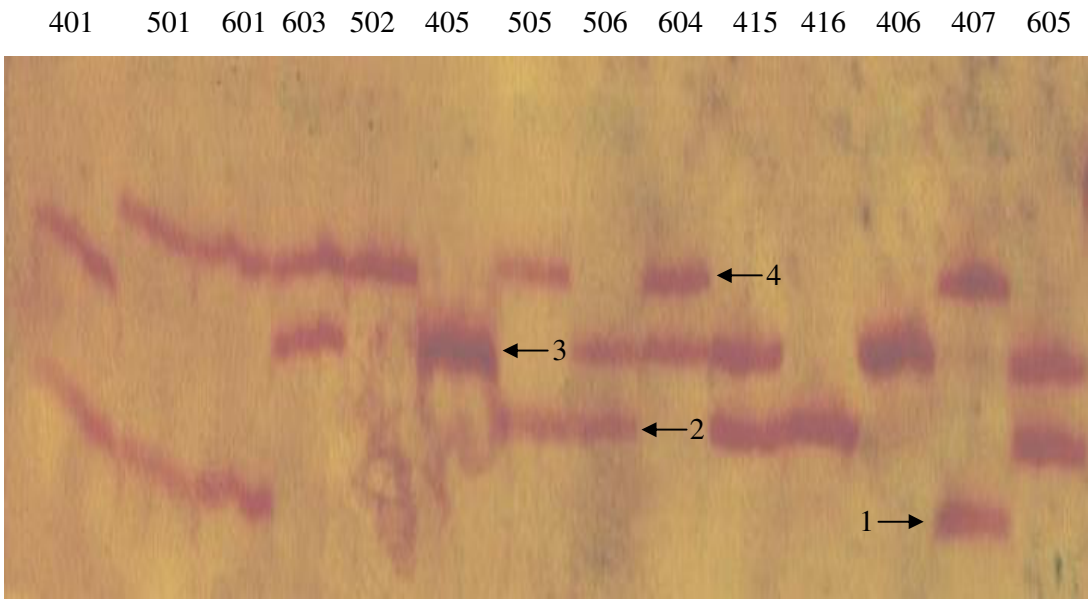

Figure 5.1. Silver-stained gel showing the alleles for D18S865 in PEMD family. Arrows show marker alleles. Numbers above designate individuals as in the pedigree

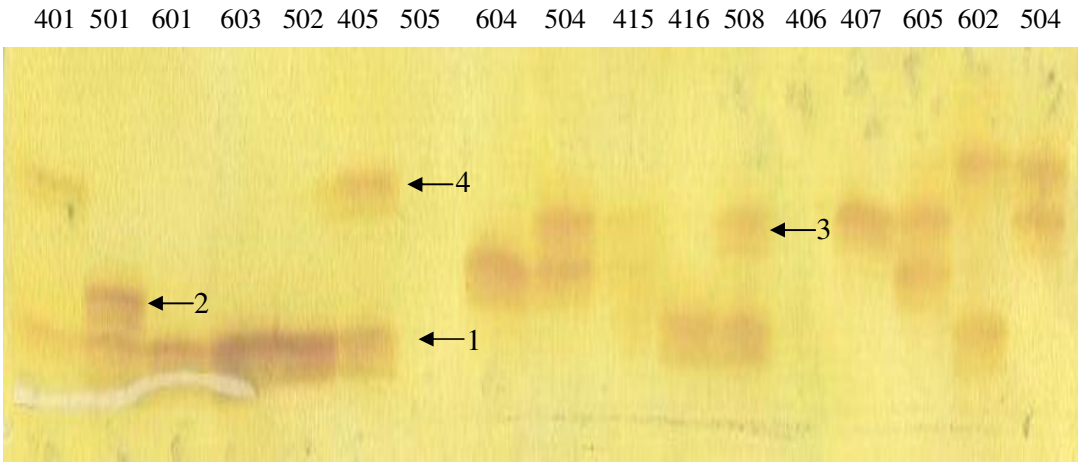

Figure 5.2. Silver-stained gel showing the alleles of D16S768 at the *ABAT* locus, in PEMD family. Arrows show marker alleles. Numbers above designate individuals as in the pedigree

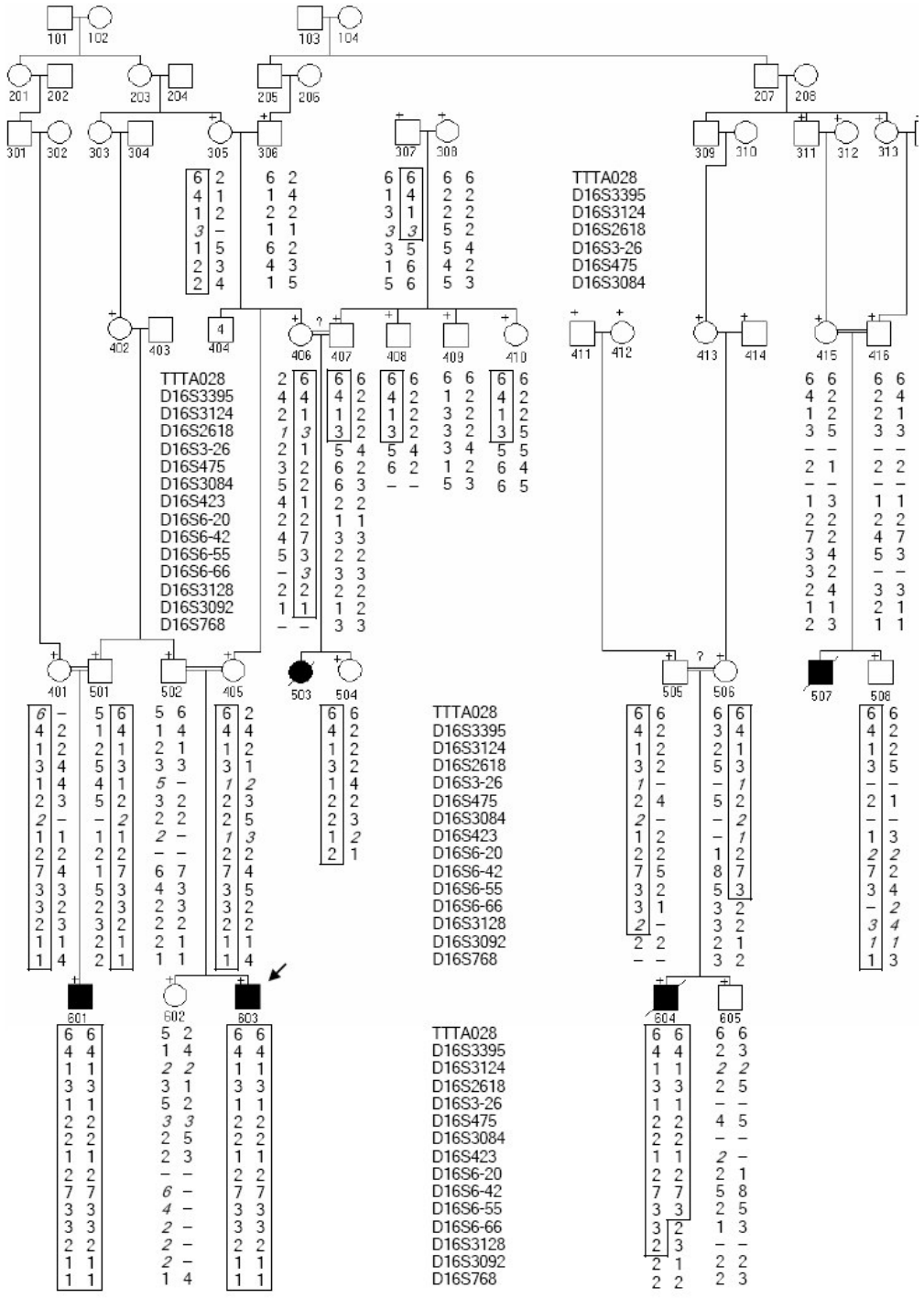

Figure 5.3. Haplotypes of PEMD family for 15 markers analyzed at 16pter. Deduced alleles are in italics. The index case is shown with an arrow

Table 5.6. Twenty-five markers used at 16pter, their physical positions, and the two-point lod scores. [a]GenBank sequence map; [b]Recombination fraction; [c]Maximum two-point lod score; [d]Maximum likelihood estimate for recombination fraction; [e]Primers designed in this study

		Lod Score at θ^b=0								
Locus	*Mbp*[a]	*0.00*	*0.001*	*0.05*	*0.1*	*0.2*	*0.3*	*0.4*	Z_{max}[c]	θ_{MLE}[d]
TTTA028	0.60	3.59	3.50	3.15	2.71	1.85	1.08	0.46	3.59	0.00
D16S3024	1.59	3.11	3.04	2.76	2.40	1.66	0.96	0.39	3.11	0.00
D16S3395	1.94	3.64	3.56	3.21	2.78	1.88	1.03	0.38	3.64	0.00
D16S3124	2.39	3.54	3.44	3.03	2.53	1.61	0.83	0.28	3.54	0.00
D16S2618	3.19	3.73	3.64	3.27	2.81	1.88	1.03	0.39	3.73	0.00
D16S3-26[e]	3.26	3.73	3.63	3.26	2.79	1.86	1.00	0.36	3.73	0.00
D16S475	3.41	3.92	3.83	3.45	2.97	1.97	1.04	0.36	3.92	0.00
D16S3084	4.21	2.30	2.20	2.00	1.80	1.20	0.70	0.30	2.30	0.00
D16S5-21[e]	5.21	3.35	3.25	2.84	2.35	1.43	0.69	0.22	3.35	0.00
D16S423	5.98	3.50	3.41	3.05	2.59	1.71	0.91	0.33	3.50	0.00
D16S6-11[e]	6.11	3.50	3.42	3.11	2.70	1.88	1.09	0.44	3.50	0.00
D16S6-20[e]	6.20	3.06	2.99	2.71	2.35	1.62	0.92	0.36	3.06	0.00
D16S2616	6.21	1.81	1.78	1.65	1.45	1.02	0.61	0.26	1.81	0.00
D16S6-23[e]	6.23	2.78	2.72	2.47	2.15	1.49	0.85	0.34	2.78	0.00
D16S3392	6.30	3.48	3.40	3.05	2.61	1.71	0.89	0.29	3.48	0.00
D16S6-42[e]	6.42	3.84	3.75	3.35	2.85	1.86	0.98	0.35	3.84	0.00
D16S6-51[e]	6.51	2.94	2.87	2.58	2.21	1.47	0.80	0.29	2.94	0.00
D16S6-55[e]	6.55	3.77	3.67	3.27	2.77	1.80	0.94	0.32	3.77	0.00
D16S6-57[e]	6.57	3.71	3.62	3.28	2.83	1.92	1.06	0.39	3.71	0.00
D16S6-66[e]	6.66	2.70	2.64	2.39	2.05	1.34	0.70	0.24	2.70	0.00
D16S3128	6.98	-1.78	0.95	1.38	1.35	0.99	0.57	0.23	1.40	0.06
D16S3088	7.15	2.58	2.53	2.33	2.05	1.44	0.84	0.34	2.58	0.00
D16S3092	7.50	3.43	3.35	3.05	2.66	1.85	1.08	0.44	3.43	0.00
D16S768	8.31	-1.48	1.22	1.59	1.48	1.00	0.52	0.18	1.59	0.05
D16S748	12.05	-7.07	-1.49	-0.27	0.11	0.27	0.22	0.11	0.27	0.21

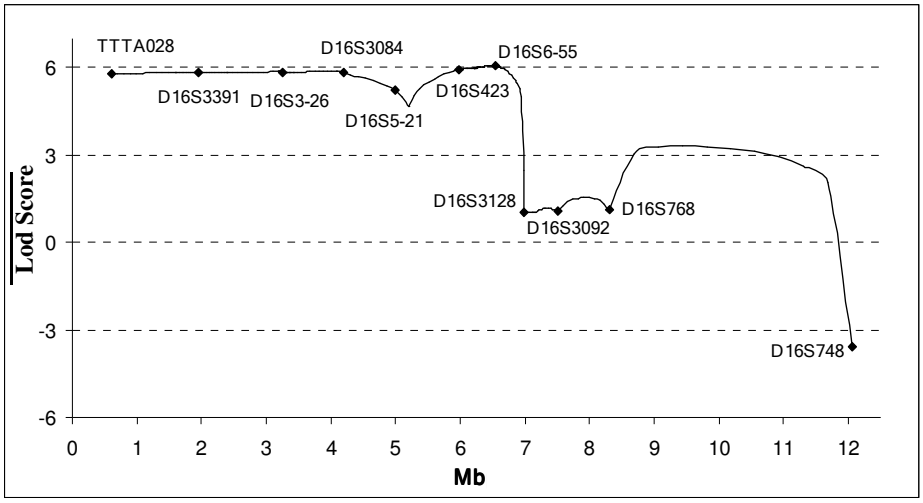

Fig 5.4. Multi-point lod score curve at 16pter. Markers used for the analysis are shown in the graph

Figure 5.5 and Figure 5.6 show the silver-stained gels for alleles of D16S2618 and D16S6.65, respectively, at 16p in PEMD family.

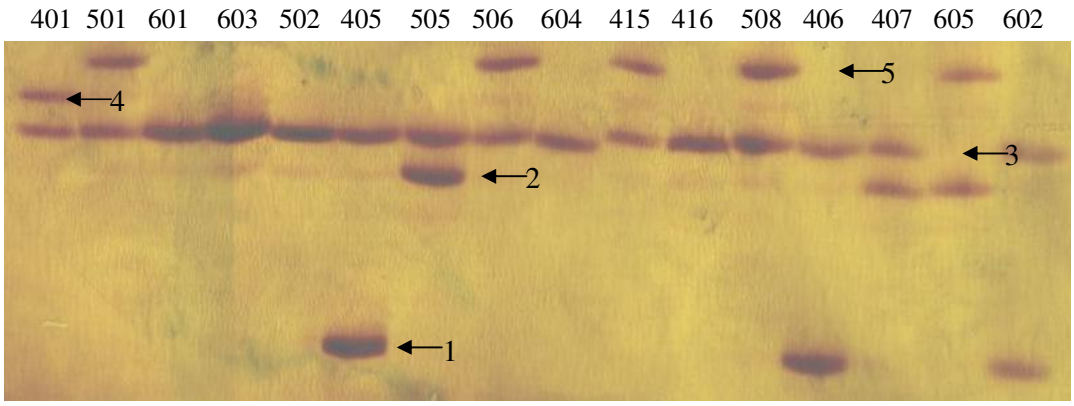

Figure 5.5. Silver-stained gel showing the alleles of D16S2618 in PEMD family. Arrows show marker alleles. Numbers above designate individuals as in the pedigree

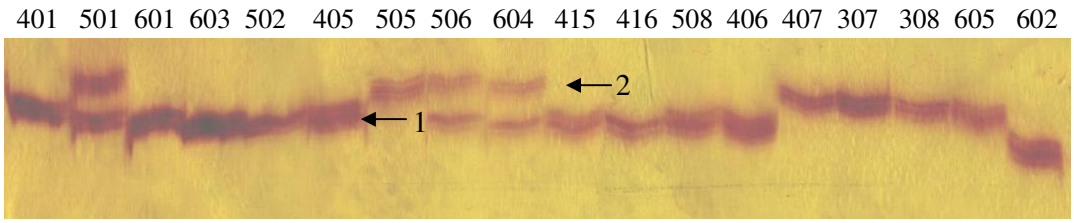

Figure 5.6. Silver-stained gel showing the alleles of D16S6-65 in PEMD family. Arrows show marker alleles. Numbers above designate individuals as in the pedigree

5.2. Linkage Analyses for INAD Families

The autozygosity mapping was carried out by using mainly the first two families. As was mentioned in the introduction, INAD shares some phenotypic properties with several neurological disorders. Therefore, the chromosomal regions of some of such diseases had been previously tested in our laboratory for Family 1 for linkage using the microsatellite markers within the loci but no homozygosity had been found (Akyüz, 2002). The diseases were Hallervorden-Spatz disease (20p13-p12), α-NAGA deficiency (22q11), chloride cahannel 1 (CLN1, 1p31), CLN2 (11p15), and CLN3 (16p12).

Within the scope of this study, the genome scan results obtained from MGS for consanguineous families 1, 2 and 3 were analyzed for a shared homozygous region in the patients, but no obvious gene locus could be detected. Also, all families were analyzed for homozygosity at D20S889, a marker about 43,000 nucleotides downstream of *PANK2*, the gene responsible for the late infantile form of the disease (Hallervorden-Spatz syndrome). None of the families was indicative of linkage to the gene locus.

In addition, nine loci were analyzed in all five families. Especially Family 1 was sufficiently large to allow gene localization; however, mapping was complicated by the inbreeding in the family. Several members of Family 3, Family 4 and Family 5, including all patients, were also analyzed together with the first two families. Pedigrees of the families are given in Figure 3.2 and Figure 3.3.

5.2.1. Linkage Analyses in INAD Family 1

Five regions on chromosomes 6, 11, 14, 7 and 8 were assessed as candidate regions that could possibly harbor the gene responsible for the INAD disease in Family 1 after the evaluation of the genome scan results. Candidate loci were fine mapped by genotyping with microsatellite markers, and candidate locus on chromosome 6 was further analyzed with SNP markers.

For Family 1 chromosome 6 appeared as the strongest candidate, since homozygous regions in the two affected individuals overlapped for several markers in a small region. The genotypes are given in Figure 5.7. The haplotypes of Family 4 at this locus is given in

Table 5.7. The haplotypes of Families 2 and 3 for markers D6S305, D6S955 and D6S411 are also given in Table 5.7. The *PARK2* (161689661bp-163068793bp), the only gene in that region, is responsible for the juvenile parkinsonism disease (JP), which is also an autosomal recessive neurodegenerative disease having some common clinical features with INAD disease. There were no polymorphic markers in the region to facilitate further fine mapping. Therefore, the locus was analyzed with SNP markers. Three markers were designed that amplified regions containing a total of 18 SNPs within the exon 6 and exon7 of *PARK2*. However, amplification with one of the primer pairs amplifying the region and containing nine SNPs could not be optimized, and sequence results of the other two revealed that they were noninformative.

The multi-point lod score analysis was performed to assess the significance of the results. A maximum lod score of 0.768 was obtained around marker D6S305, where *PARK2* gene lied. Being between -2 and 3, the lod score was inconclusive.

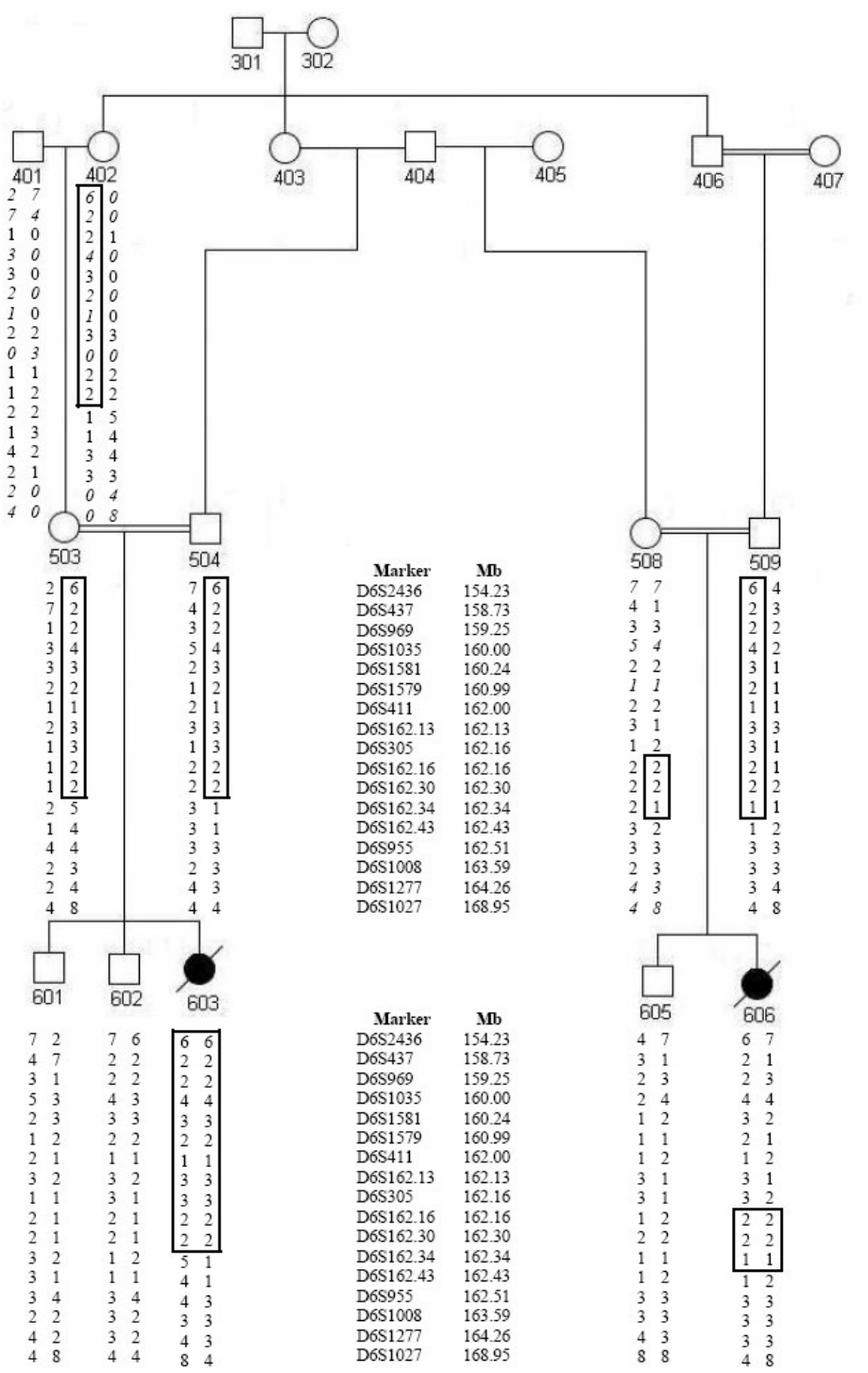

Figure 5.7. The haplotypes of INAD Family 1 in candidate region at chromosome 6q25.2-q26

Table 5.7. Haplotypes of Family 4 at 6q25.2-q26

Family		**4**				**2**				**3**		
Individual		**101**	**102**	**201**	**202**	**201**	**202**	**301**	**302**	**202**	**201**	**301**
ID		**M**	**F**	**P1**	**P2**	**M**	**F**	**P1**	**P2**	**M**	**F**	**P**
MARKER	**POSITION (Mb)**											
D6S969	159.25	2 2	1 1	2 2	1 2	-	-	-	-	-	-	-
D6S1581	160.24	2 2	2 2	2 2	2 2	-	-	-	-	-	-	-
D6S411	162.00	1 1	1 2	1 1	1 2	2 2	1 2	2 2	1 2	1 1	2 2	1 2
D6S162.13	162.13	2 2	1 2	-	-	-	-	-	-	-	-	-
D6S305	162.16	1 3	3 3	3 3	3 3	3 3	3 3	3 3	3 3	1 2	1 3	1 3
D6S162.16	162.16	1 2	1 2	1 2	1 1	-	-	-	-	-	-	-
D6S162.20	162.20	1 1	1 2	1 1	-	-	-	-	-	-	-	-
D6S162.30	162.30	1 2	2 2	1 2	1 2	-	-	-	-	-	-	-
D6S162.34	162.34	2 2	3 4	2 3	2 4	-	-	-	-	-	-	-
D6S162.43	162.43	2 2	1 3	1 2	2 3	-	-	-	-	-	-	-
D6S955	162.51	-	1 3	3 3	1 3	3 4	3 4	3 4	3 4	1 1	1 3	1 3
D6S1008	163.59	2 3	2 2	2 2	2 2	-	-	-	-	-	-	-
D6S163-67	163.67	-	-	-	-	-	-	-	-	-	-	-

Figure 5.8 and 5.9 show the silver-stained gels for alleles of D6S969 and D6S162.16 at 6q in INAD families.

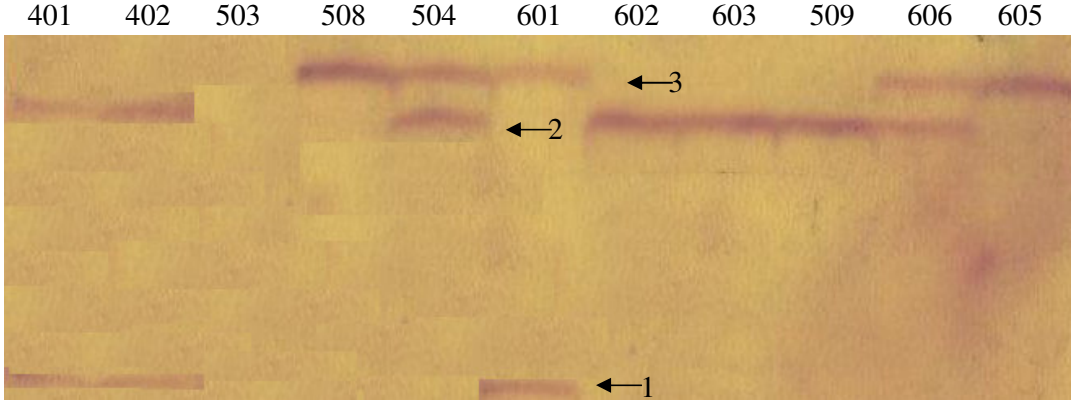

Figure 5.8. Silver-stained gel showing the alleles of D6S969 in INAD Family 1. Arrows show marker alleles. Numbers above designate individuals as in the pedigree

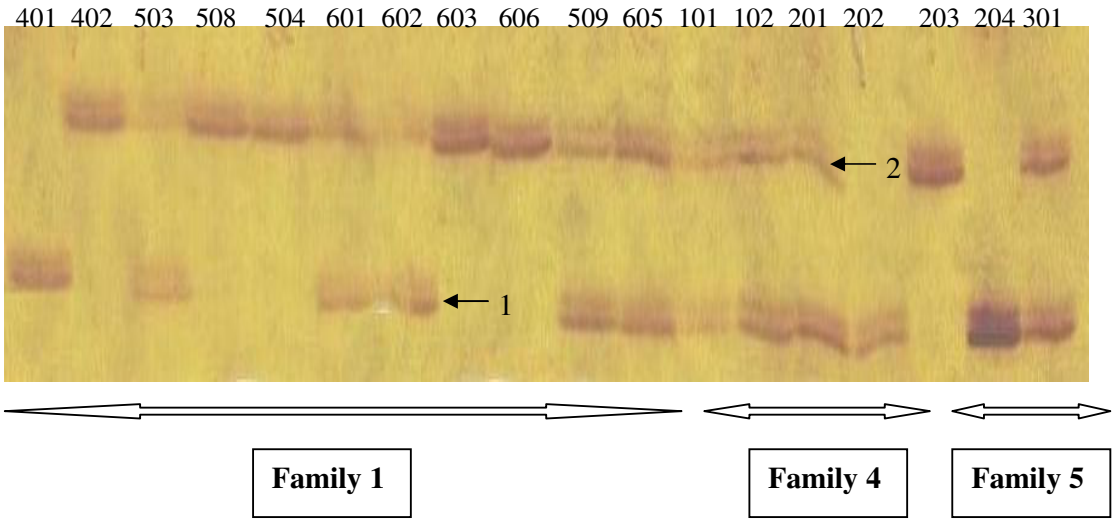

Figure 5.9. Silver-stained gel showing the alleles of D6S162.16 in INAD Families 1, 4 and three individuals of Family 5. Arrows show marker alleles. Numbers above designate individuals as in the pedigree

The region on chromosome 11 seemed a strong candidate, since the two affected individuals shared a common homozygous region. The fact that the mother of one affected individual also carried the homozygous region posed a problem; however, the region could not be excluded, considering that the disease might be digenic. The genotypes are given in Figure 5.10. The haplotypes of Family 4 at this locus is given in Table 5.8.

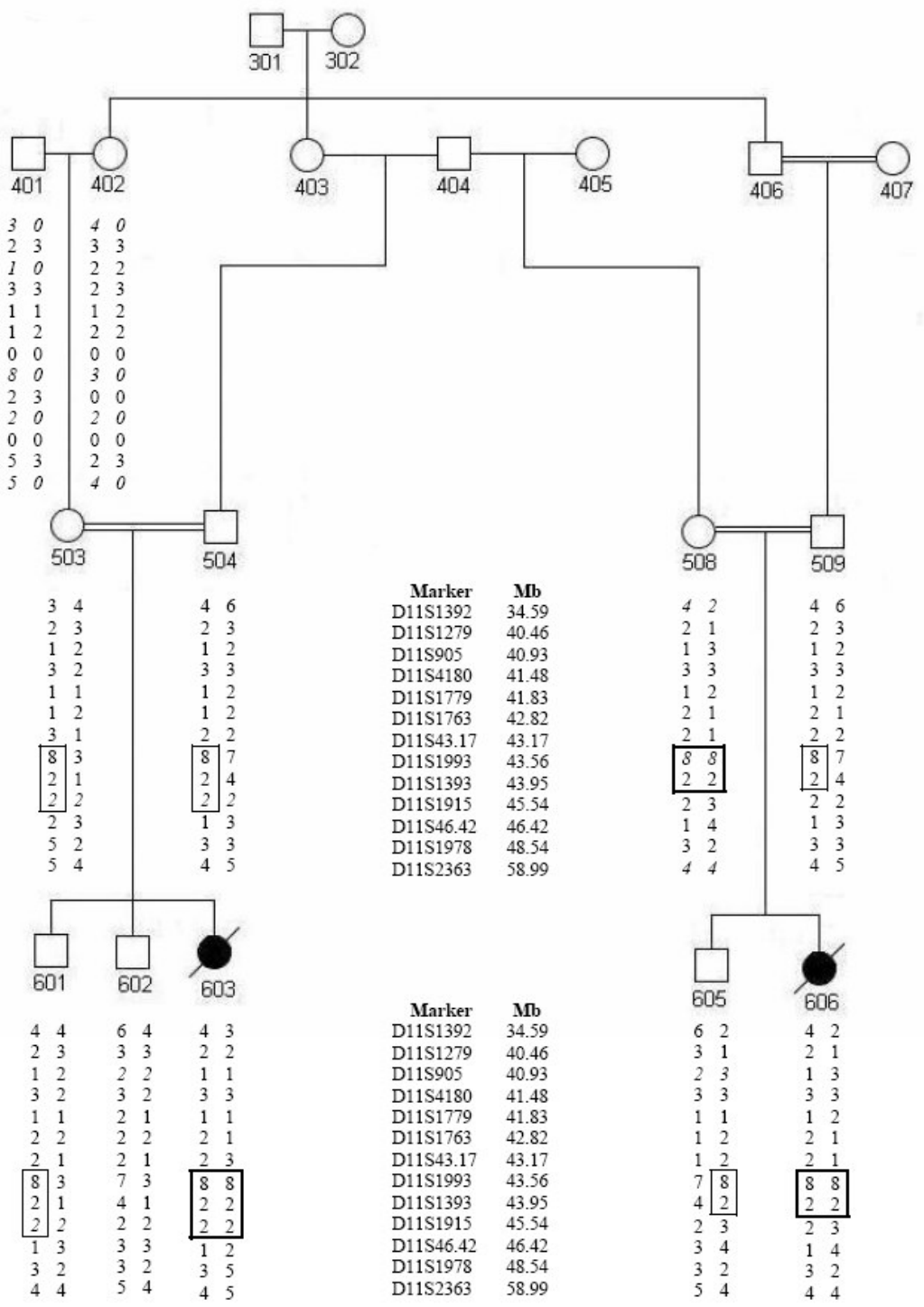

Figure 5.10. The haplotypes of INAD Family 1 in candidate region at chromosome 11p13-q12.1

Table 5.8. Haplotypes of Family 4 at 11p13-q12.1

Family		**4**			
Individual		**101**	**102**	**201**	**202**
ID		**M**	**F**	**P1**	**P2**
MARKER	**POSITION (Mb)**				
D11S1279	40.46	3 3	3 3	-	3 3
D11S905	40.93	-	1 1	1 1	1 3
D11S4180	41.48	2 3	-	-	2 2
D11S1763	42.82	2 2	2 2	2 2	2 2
D11S43.17 [d]	43.17	2 2	1 2	-	1 2
D11S1393	43.95	-	2 2	-	2 3
D11S46.42 [d]	46.42	1 2	1 1	-	-
D11S1978	48.54	1 2	1 2	-	2 2

Chromosome 14 was excluded after autozygosity mapping, since no homozygous block shared by affected individuals was found. Table 5.9 shows the haplotypes of two patients and their parents in Family 1 and the haplotypes of Family 4 at 14q32.

Table 5.9. The haplotypes of the patients and their parents in Family 1 and Family 4 at 14q32.13-q32.33

Family		**1**						**4**			
Individual		**508**	**509**	**606**	**503**	**504**	**603**	**101**	**102**	**201**	**202**
ID		**M**	**F**	**P**	**M**	**F**	**P**	**M**	**F**	**P1**	**P2**
MARKER	**POSITION (Mb)**										
D14S617[*]	91.27	*3 0*	*2 2*	2 3	*6 2*	2 2	2 2	-	-	-	-
D14S1434[*]	-	*2 0*	3 4	3 2	*3 1*	2 3	3 3	-	-	-	-
ATGG002[*]	-	*2 3*	4 2	4 2	*4 3*	2 4	4 4	-	-	-	-
G09851	100.43	2 2	2 1	2 2	2 2	1 2	2 2	-	-	-	-
D14S100.72 [d]	100.72	3 2	3 3	3 3	2 4	2 2	2 2	1 4	2 5	4 5	1 2
D14S543	103.65	1 2	2 4	2 1	4 2	5 1	2 1	-	-	-	-
ATT168Z[*]	-	*3 2*	4 3	4 3	*0 3*	4 3	3 3	-	-	-	-

Since a homozygous region shared by the affected individuals was not found, the region on chromosome 7 did not seem a strong candidate locus. Table 5.10 shows the haplotypes of two patients and their parents in Family 1 and Family 4.

Table 5.10. The haplotypes of the patients and their parents in Family 1 and Family 4 at 7q36.1-q36.3

Family		**1**						**4**			
Individual		**508**	**509**	**606**	**503**	**504**	**605**	**101**	**102**	**201**	**202**
ID		**M**	**F**	**P**	**M**	**F**	**P**	**M**	**F**	**P1**	**P2**
MARKER	**POSITION (Mb)**										
GATA104*	**-**	-	*3 7*	3 4	*2 3*	4 3	4 3	-	-	-	-
D7S3070*	150.52	*6 4*	6 4	6 4	*7 6*	6 4	6 7	-	-	-	-
D7S1815	151.83	2 4	2 3	2 4	3 2	2 2	2 2	3 3	3 3	3 3	3 3
GATA2C08	152.43	1 2	1 1	1 2	1 2	1 1	1 1	2 3	3 3	2 3	3 3
D7S1823*	153.42	*4 4*	*4 3*	4 3	*0 4*	4 3	4 4	-	-	-	-
D7S550	155.01	1 1	1 2	1 2	1 1	1 1	1 1	-	-	-	-
MFD442-GTTT002*	155.41	*2 2*	2 4	*2 2*	*0 2*	2 1	2 2	-	-	-	-

After fine mapping of the candidate locus on chromosome 8, this region was also excluded. The results revealed that there was no homozygous region shared by the patients. Table 5.11 shows the haplotypes of the patients and their parents in Family 1 and Family 4.

Table 5.11. The haplotypes of thepatients and their parents in Family 1 and Family 4 at 8p23.2-p23.1

Family		**1**						**4**			
Individual		**508**	**509**	**606**	**503**	**504**	**605**	**101**	**102**	**201**	**202**
ID		**M**	**F**	**P**	**M**	**F**	**P**	**M**	**F**	**P1**	**P2**
MARKER	**POSITION (Mb)**										
ATT023*	4.13	*4 0*	4 4	4 4	*4 0*	4 4	4 4	-	-	-	-
D8S1798	5.08	3 1	1 1	1 3	1 3	*3 0*	3 1	-	1 1	1 1	1 2
TTCA004P*	9.16	*4 0*	4 4	4 4	*4 0*	4 4	4 4	-	-	-	-
D8S11086	9.18	1 1	2 2	1 2	1 2	1 1	1 1	2 3	1 2	2 2	1 2
ATT070*	14.96	*4 0*	*3 7*	3 4	*7 0*	7 3	7 7	-	-	-	-
ATAA018P*	-	*3 0*	3 3	3 3	*3 2*	4 3	4 3	-	-	-	-

5.2.2. Linkage Analyses in INAD Family 2

Three regions on chromosomes 2, 18 and 21 were assessed as candidate regions that may possibly harbor the gene responsible for INAD in Family 2 after the evaluation of the genome scan results data. The candidate loci were analyzed using microsatellite markers reported by Marshfield and with primers designed within the framework of this study. The candidate locus for Family 1 on chromosome 6 was analyzed for this family as well using markers D6S980, D6S305, D6S955 and D6S411.

Genotyping at the candidate region on chromosome 2 revealed that patients were homozygous for two markers at the locus. However, heterozygosity was found between these two markers. The region will further be investigated. Table 5.12 shows the haplotypes of the patients and their parents in Family 2.

Table 5.12. The haplotypes of the patients and their parents in Family 2 at 2q37.1-q37.3

Family		**2**			
Individual		**301**	**302**	**401**	**402**
ID		**M**	**F**	**P1**	**P2**
MARKER	**POSITION (Mb)**				
D2S1363*	226.74	*6 4*	4 2	4 4	4 6
D2S427*	232.03	*3 3*	3 4	3 3	3 3
D2S2348	233.93	1 2	2 3	2 1	2 1
GATA23A02*	-	*2 3*	2 1	2 2	2 2
D2S338	237.01	1 3	2 3	3 1	3 1
D2S2968*	237.86	*2 0*	2 4	2 2	2 2
AGAT021*	-	*4 0*	2 3	2 4	2 4

The fine mapping of the candidate region on chromosome 21 revealed that patients were not sharing a homozygous region. Therefore, the region was excluded. Table 5.13 shows the haplotypes of the patients and their parents in Family 2 and Family 4. Figure 5.11 shows the silver-stained gel for alleles of D21S1235 in Family 1.

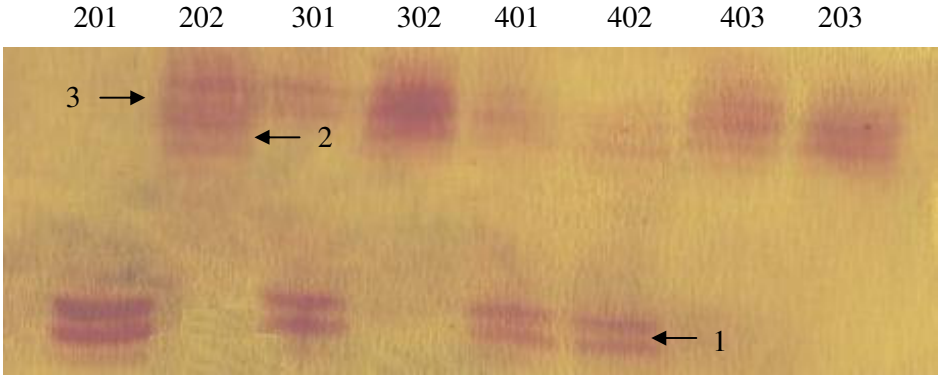

Figure 5.11. Silver-stained gel showing the alleles of D21S1235 in INAD Family 2. Arrows show marker alleles. Numbers above designate individuals as in the pedigree.

Table 5.13. The haplotypes of the patients and their parents in Family 2 and Family 4 at 21q22.13-q22.3

Family		**2**				**4**			
Individual		**301**	**302**	**401**	**402**	**101**	**102**	**201**	**202**
ID		**M**	**F**	**P1**	**P2**	**M**	**F**	**P1**	**P2**
MARKER	**POSITION (Mb)**								
D21S2052*	27.74	*4 6*	*6 3*	6 4	3 4	-	-	-	-
D21S1440*	38.06	*2 2*	2 2	2 2	2 2	-	-	-	-
D21S1809	38.81	2 2	1 1	1 2	1 2	3 3	2 2	2 3	2 3
D21S2055*	40.11	*2 1 3*	2 2	2 2	2 1 3	-	-	-	-
D21S1235	41.38	1 3	3 3	3 1	3 3	-	-	-	-
D21S1411*	43.03	6 8	6 6	6 8	6 8	-	-	-	-
D21S1446*	43.03	8 7	2 4	2 7	2 7	-	-	-	-

Chromosome 18 was excluded after genotyping at the candidate region, since no shared homozygosity was found. Table 5.14 shows the haplotypes of the patients and their parents in Family 2 and Family 4. Figure 5.12 shows the silver-stained gel containing the alleles of D18S865 in Families 2 and 4.

Table 5.14. The haplotypes of the patients and their parents in Family 2 and Family 4 at 18q12.3-q21.1

Family		**2**				**4**			
Individual		**301**	**302**	**401**	**402**	**101**	**102**	**201**	**202**
ID		**M**	**F**	**P**	**P**	**M**	**F**	**P1**	**P2**
MARKER	**POSITION (Mb)**								
G10491	35.73	2 2	3 1	2 3	2 3	-	-	-	-
D18S535*	36.40	5 2	2 5	2 2	2 2	-	-	-	-
D18S865	36.59	3 3	1 3	3 1	3 1	-	2 4	2 2	2 4
D18S851*	48.36	3 4	2 2	3 2	3 2	-	-	-	-

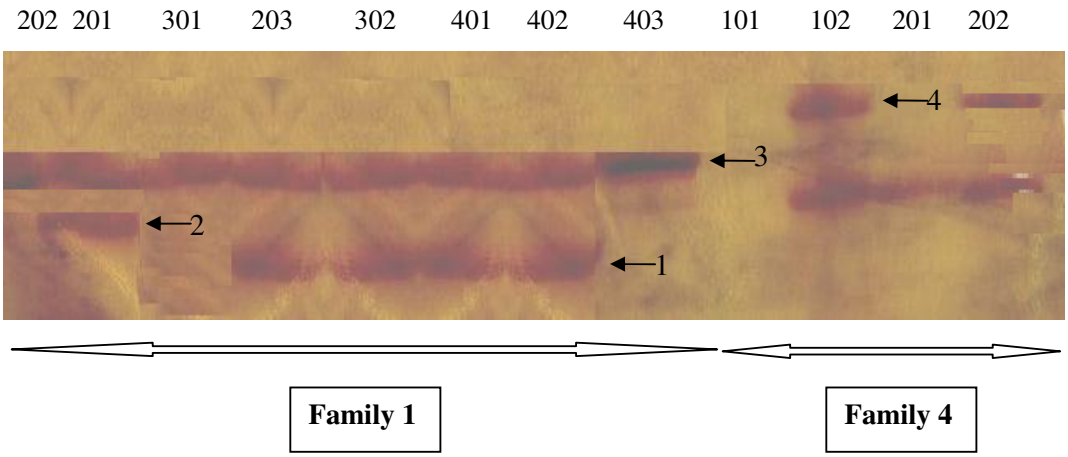

Figure 5.12. Silver-stained gel showing the alleles of D18S865 in INAD Families 2 and 4. Arrows show marker alleles. Numbers alone designate individuals of the family

5.2.3. Linkage Analyses in INAD Family 3

A region on chromosome 8 was identified as a candidate locus that could possibly harbor the gene responsible for the INAD disease in Family 3 after the evaluation of the genome scan results. The candidate locus was fine mapped with microsatellite markers reported by Marshfield. The candidate locus for Family 1 on chromosome 6 was also analyzed for this family with markers D6S980, D6S305, D6S955 and D6S411. An example of a silver-stained gel showing the alleles of D6S980 in Family 3 is given in Figure 5.13.

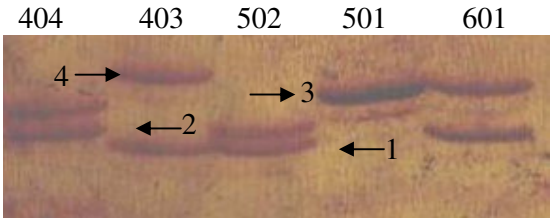

Figure 5.13. Silver-stained gel showing the alleles of D6S980 in INAD Family 3. Arrows show marker alleles. Numbers above designate individuals as in the pedigree.

Genotyping at the candidate region on chromosome 8p revealed that the patient in Family 3 had a homozygous block for three markers. Both parents were informative for the markers. The region needs to be analyzed further with additional markers. Table 5.15 shows the haplotypes of the patients and their parents in Family 3 and Family 4.

Table 5.15. The haplotypes of the patients and their parents in Famiy 3 and Family 4 at 8p21.2-p12

Family		**3**			**4**			
Individual		**502**	**501**	**601**	**101**	**102**	**201**	**202**
ID		**M**	**F**	**P**	**M**	**F**	**P1**	**P2**
MARKER	**POSITION (Mb)**							
TTA024*	-	1 3	3 2	3 1	-	-	-	-
D8S1048*	26.87	4 5	4 5	4 4	-	-	-	-
D8S1809	28.24	4 2	4 3	4 4	2 3	1 3	1 3	1 3
D8S1477*	32.18	6 1	6 2	6 6	-	-	-	-
D8S1110*	53.34	2 2	1 2	1 2	-	-	-	-

6. DISCUSSION

In this study, the gene responsible for one disease was localized, while the other one was not, despite analyses of several candidate loci.

6.1. Early Onset Progressive Encephalopathy with Myoclonus and Dystonia

The first disorder studied was PEMD. The aim was first to identify the gene locus for this autosomal recessive neurological disease observed in the single large inbred PEMD family by using autozygosity mapping strategy and later to identify the candidate genes in the locus. After fine mapping at the candidate locus at 16p.13 and lod score analysis, genetic linkage to the locus was ascertained and the gene responsible for the disease was localized to a maximum 3.26 Mb-interval on chromosome 16p.

The three affected individuals from whom DNA samples were available were found to share a large homozygous block within the 6.66 Mb-interval beginning from the telomere at 16p. The parents of two other affected individuals whose DNA samples were unavailable were also investigated and were found to carry the disease haplotype. Such a shared homozygosity was consistent with descent from a common ancestor, although the blood relation was not known for all parents. Lod scores were calculated to assess the significance of the result, and they supported the haplotype data. Two-point linkage analysis yielded lod scores higher than 3.00 at a recombination fraction of zero for most of the markers in the region spanning 0 – 6.98 Mbp. Multi-point lod score curved up around 6 from 16pter to 6.66 Mb. However, an ancestral crossover event in individual 407 telomeric to D16S3-26 was detected by haplotype analysis, and this narrowed down the gene locus to a 3.26 Mbp interval at 16pter. The linkage programs did not take into consideration the haplotype data of the family. The reasons were that the presumable consanguinity between individuals 406 and 407 could not be presented to the linkage programs and only the DNA of a single child was available from that branch of the family. Thus, the programs could not extract any linkage information from this core family.

The region between D16S2616 and D16S748 was genotyped with an unusually high member of markers. The reason of such genotyping was that when genotyping data was sent to our laboratory from Marshfield, the first marker on chromosome 16 was reported as ATA3A07. However, GenBank placed ATA3A07 to 12.05 Mb, which made it the third marker in the map. Since this inconsistency was not noticed earlier, the region was genotyped with tight markers.

The gene locus at 16pter contains 173 genes, 25 of which could be assigned as candidate genes. They can be grouped according to function as follows: (1) metabolic enzymes: *ATP6V0C*, *CGI-14*, *DCI*, *DECR2*, *DKFZP566J2046*, *HAGH*, *HAGHL*, *LOC440332*, *MGC2655*, *PIGQ* and *TSC2*; (2) Rab GTPases and their regulators: *RAB26*, *RAB40C*, *RAB11FIP3* and *ARHGDIG*; (3) Heterotrimeric G protein subunits and their regulators: *GBL* and *RGS11*; (4) G protein coupled receptors and their ligands: *SSTR5* and *PPL8*; (5) gene products that may lead to neurodegeneration: *STUB1*, *AXIN1* and *KREMEN2*; (6) subunit of NADH dehydrogenase (ubiquinone) 1 beta subcomplex: *NDUFB10*; (7) a MAP kinase: *MAPK8IP3*; and (8) a neuronal integral membrane protein *SYNGR3*. Whether any of the genes at the locus could be a candidate gene for a myoclonic dystonia-like disease was also investigated. Unlike the PEMD disease, myoclonic dystonia disease (MIM 159900) is a mild condition that is inherited as an autosomal dominant trait with incomplete penetrance. Nevertheless, the related genes in the identified gene locus deserve mentioning. Myoclonic dystonia disease was shown to result from mutations in *epsilon sarcoglycan* (*SGCE*) at 7q21 (Zimprich *et al.*, 2001; Asmus *et al.*, 2002), but additionally *DR dopamine receptor* (*DRD2*) (Klein *et al.,* 1999) or *torsin-A* (*TOP1A*) (Ozelius *et al.*, 1997; Leung *et al.*, 2001) mutations were found to be associated with it. One of the genes located at the gene locus is the somatostatin receptor (SSTR5) that interacts physically with DRD2 (Rocheville *et al*., 2000). Somatostatin (SST) is a major neurotransmitter system with similarities to that of dopamine. It has a role in the modulation of dopamine-mediated control of motor activity. Torsin-A is a member of the ATPases associated with various cellular activities (AAA) family. It was found to be highly expressed in substantia nigra (Konakova *et al.*, 2001). Another gene having high expression in substantia nigra, thus a good candidate, is *Preproneuropeptide W* at the PEMD locus.

Several other neurological diseases manifesting epileptic seizures have already been localized to the gene locus. Zara *et al*. (2000) identified an idiopathic epilepsy disease mapping to 16p13, which also manifests with myoclonic seizures in 8 patients belonging to a large Italian family (MIM 605021, Myoclonic epilepsy, infantile). The gene was mapped to 1.59 - 5.98 Mb, overlapping with the PEMD locus. Nevertheless, this infantile myoclonic epilepsy does not present the typical clinical features in PEMD patients who have much severe phenotypes: a progressive course and developmental and neurological retardation that together with systemic infections lead to a full deterioration. In spite of these differences, there are some common clinical features including the presence of fever induced seizures, infantile onset of myoclonia, and relative scarcity of EEG abnormalities, indicating some overlaps between these two syndromes. However, even in the 3.26 Mb-interval, there are as many as 173 genes. Several of them appear as candidate genes, which if defected might lead to a disorder similar to PEMD. Also, we do not exclude the possibility that different mutations in the same gene may lead to these two disorders sharing some clinical properties; a more severe mutation may lead to PEMD disease with more severe manifestations. Nevertheless, we cannot state that they are definitely the same disorder; taking into consideration several different phenotypic features and the abundance of candidate genes at the gene locus. Two other diseses mapping to the locus is also associated with epilepsy. Guerrini *et al*. (1999) reported linkage to 16p12 in an inbred family affected by rolandic epilepsy, paroxysmal exercise-induced dystonia and writer's cramp. Chen *et al*. (2003) found 12 missense mutations in the coding region of *CACNA1H* gene located at 16p13.3 in patients with Childhood Absence Epilepsy (CAE). These studies support the idea that different genes in the same locus could lead to disorders with common clinical features. It can be suggested that the chromosome 16 possibly harbors a gene family. Mutations in members of such a family could be associated with different epilepsy phenotypes, paroxysmal disorders and dystonia. Furthermore, as suggested by Zara *et al*. (2000), among the myoclonic epilepsies of infancy, clinical overlap is widely seen. The diagnostic classification of infancy/early childhood epilepsies characterized by myoclonic seizures has always been difficult due to the clinical heterogeneity.

Recently Pinto *et al*. (2005) also mapped a gene to this locus for families afflicted with myoclonic seizures. The patients in all families had photosensitivity (photoparoxysomal response or photosensitivity in EEG, PPR) which showed a prominent

myoclonic seizures background. Patients reported by Zara *et al.*(2000) also showed EEG abnormalities under photic stimulation. However, in the PEMD family we studied, there was no photosensitivity in the affected individuals.

We believe that the disease in patients we studied is novel with unique clinical features and can best be described as a very severe, autosomal recessive form of infantile onset progressive myoclonus epilepsy associated with paroxysmal and then persistent dystonia. Other symptoms of extrapyramidal, pyramidal, autonomic and cognitive involvement of the nervous system with initially paroxysmal but later persistent manifestations might lead to eventual death.

Common infections played a significant role in exacerbating the clinical status of the patients. Absence of laboratory evidences of likely etiologies suggested a possible disorder of hereditary metabolic origin not detectable by standard screenings. In the absence of a definite diagnosis for Patient 603 just after referral, the infantile form of neuronal ceroid lipofuscinosis had been investigated by skin biopsy. The result was negative. Furthermore, there are no known genes of the disease in the locus we identified.

Although the molecular basis for this new syndrome with predominantly myoclonic and dystonic features remains unidentified, the localization of a gene responsible for the novel disorder would have benefits for families afflicted with diseases exhibiting similar clinical features, as they can be tested for linkage to the locus.

The future goal for PEMD project is to screen several candidate genes for mutations. At present the strongest candidate seems to be *SSTR5*, and we are planning to analyze for mutations in patients with priority.

6.2. Infantile Neuroaxonal Dystrophy

The second disease studied within the framework of this thesis was INAD. As was mentioned in the introduction, there are several other neurological disorders that exhibit similar clinical characteristics with the disease, and there are some criteria suggested by Aicardi for its diagnosis. Nevertheless, clinical heterogeneity still presents a problem for

the diagnosis of the disease. Because high heterogeneity was also detected among the patients of INAD families, the genetic loci for other neurological disorders showing similar clinical features had been previously tested for genetic linkage (Akyüz, 2002). As a result, they were all excluded. During this study, taking into consideration the clinical heterogeneity, the PANK2 gene was also tested for linkage for all INAD families, and none of the families was found indicative of linkage to the gene locus.

Homozygosity mapping strategy was applied to identify the locus that could harbor the gene responsible for INAD disease. The candidate locus for INAD Family 1 at 6q25.2-q26 seemed interesting. The two affected individuals have homozygous blocks within the locus, but these blocks overlapped at only a very short region that harbored just one gene, *PARK2*, coding the parkin protein. *PARK2* is an attractive candidate gene since defects could possibly be responsible for the disease.

PARK2 causes Juvenile Parkinsonism disease (JD), which is also an autosomal recessive neurodegenerative disease having some common clinical features with INAD. It is expressed in neuronal processes and cell bodies of neurons but not in glial cells, the midbrain, basal ganglia, cerebral cortex, and cerebellum. Several studies suggested that parkin had a role in modifying synaptic vesicle trafficking at the presynaptic terminal. Similar to INAD patients, JD patients have iron accumulation in their brains, and there are several speculations to explain the role of parkin gene in this phenomenon. Taking into consideration all similarities between JD and INAD, *PARK2* gene appears as a candidate gene.

The multi-point lod score analysis was performed to assess the significance of the homozygous region shared by the two patients. A maximum lod score of 0.768 was obtained around marker D6S305, where *PARK2* gene lies. Being between -2 and 3, the lod score was inconclusive, and the region was not excluded.

Since there were no markers or repeated sequences as candidates for polymorphic markers flanking the short candidate region, SNPs within the exons 6 and 7 of *PARK2* were utilized for fine mapping. However, they were either non-informative or the sequence

results were not clear. Therefore, the future goal is to analyze the two exons of *PARK2* that reside in the maximum homozygous region for mutations.

Although not as strong, chromosome 11 appeared as another candidate region for harboring the gene responsible for INAD. At this locus a short homozygous region was found to be shared by two patients. However, the mother of one affected individual also had the same genotype. The region could not be excluded and is still considered a candidate locus. The reason is that the disease might be digenic and mutations in at least two genes might be the cause of the disease. Despite intensive efforts of several research teams, the disease gene has not been localized yet. The diagnosis of the disease is very difficult, one reason being that there is much phenotypical variation. Each INAD child may have a different combination of clinical manifestations. These clinical features that occur in some patients but are absent in others support the proposal that more than one gene could contribute to the disease.

As a result of the analysis performed to identify the genetic locus (loci) harboring the gene responsible for INAD, no significant genetic linkage to any locus was detected. One of the reasons of this situation could be the average spacing of 8 cM between the polymorphic markers used in autozygosity mapping. Although 8 cM is not a very wide space, we might still not be enable to detect the homozygous regions. Moreover, although we had five INAD families, only two of them were sufficiently large to be informative for analysis. Small families could contribute to the lod score analysis, since the lod scores can be summed, but this is valid for only a disease with a single genetic locus. For the INAD case, on the other hand, it is strongly suggested that defects in more than one gene may lead to the disorder. Such genetic heterogeneity is most likely, because clinical heterogeneity is frequently coupled with genetic heterogeneity.

The future goal for INAD project is to further investigate the candidate loci that could possibly harbor a homozygous region and to screen candidate genes. Furthermore, Family 4 was recently sent to Marshfield for genome scan, and we hope that the results will help us identify other candidate loci. Finding the gene would enable us to understand the biochemical and pathological basis of the disease, which further could enable

researchers to search therapies to improve the lives of children with INAD disease and to perform prenatal diagnosis.

REFERENCES

Aicardi J and P. Castelein, 1979, "Infantile Neuroaxonal Dystrophy", *Brain*, Vol. 102, pp. 727-748.

Asmus, F., A. Zimprich, S. Tezenas du Montcel, C. Kabus, G. Deuschl, A. Kupsch, U. Ziemann, M. Castro, A.A. Kuhn, T.M. Strom, M. Vidailhet, K.P. Bhatia, A. Durr, N.W. Wood, A. Brice and T. Gasser, 2002, "Myoclonus-Dystonia Syndrome: Epsilon Sarcoglycan Mutations and Phenotype", *Annual Neurology*, Vol. 52, pp. 489-492.

Akyüz E.İ., 2002, *Genetic Analysis in Four Neurological Disorders*, PhD. Dissertation, Boğaziçi University.

Başaran, N., S. Saylı, A. Başaran, M. Solak, S. Artan and J. Stevenson, 1998, "Consanguineous Marriages in the Turkish Population", *Clinical Genetics*, Vol. 34, pp. 339-341.

Chen Y., L. Jianjun, P. Hong, Z. Yuehua, W. Husheng, X. Keming, L. Xiaoyan, J. Yuwu , B. Xinhua, Y. Zhijian, D. Keyue, L.H.Y. Wilson, Q Boqin, C. Piu, S. Yan and W. Xiru, 2003, "Association between Genetic Variation of *CACNA1H* and Childhood Absence Epilepsy", *Annals of Neurology*, Vol. 54, pp. 239-243.

Cottingham, R. W., R. M. Idury and A. A. Schaffer, 1993, "Fast Sequential Genetic Linkage Computations", *American Journal of Human Genetics*, Vol. 53, pp. 252-263.

Donis-Keller, H., P. Green, C. Helms, S. Cartinhour, B. Weiffenbach, K. Stephens, T. P. Infantile Neuroaxonal Dystrophy", Genetic Counsel, Vol. 13, pp. 465-473. Keith, D. W. Bowden, D. R. Smith and E. S. Lander, 1987, "A Genetic Linkage Map of the Human Genome", *Cell*, Vol. 51, pp. 319-37.

Elejalde, B.R., M.M.J. de Elejalde and F. Lopez, 1979, "Hallervorden-Spatz Disease", *Clinical Genetics*, Vol. 16, pp. 1-18.

Forshew T. and C. A. Johnson, 2004, SCAMP: "A Spreadsheet to Collate Autozygosity Mapping Projects", *Journal of Medical Genetics*, Vol. 41, pp. 125.

Gordon N., 2002, "Pantothenate Kinase-Associated Neurodegeneration (Hallervorden–Spatz syndrome)", *European Journal of Pediatric Neurology*, Vol.6, pp. 243–247.

Guerrini R, P. Bonanni, N. Nardocci, L. Parmeggiani, M. Piccirilli, M. De Fusco, P. Aridon, A. Ballabio, R. Carrozzo and G. Casari, 1999, "Autosomal Recessive Rolandic Epilepsy with Paroxysmal Exercise-Induced Dystonia and Writer's Cramp: Delineation of the Syndrome and Gene Mapping to Chromosome 16p12-11.2", *Annuals Neurology*, Vol. 45, pp. 344.

Guilford, P., S. Ben Arab, S. Blanchard, J. Levilliers, J. Weissenbach, A. Belkahia and C. Petit, 1994, "A Nonsyndromic Form of Neurosensory, Recessive Deafness Maps to the Pericentromeric Region of Chromosome 13q", *Nature Genetics*, Vol. 6, pp. 24-28.

Hortnagel, K., H. Prokisch and T. Meitinger, 2003, "An Isoform of hPANK2, Deficient in Pantothenate Kinase-Associated Neurodegeneration, Localizes to Mitochondria", *Human Molecular Genetics*, Vol. 12, pp. 321-327.

Hortnagel, K., N. Nardocci, G. Zorzi, B. Garavaglia, E. Botz, T. Meitinger and T. Klopstock, 2004, "Infantile Neuroaxonal Dystrophy and Pantothenate Kinase-Associated Neurodegeneration: Locus Heterogeneity", *Neurology*, Vol. 63, pp. 922-924.

Jaeken, J., P Casaer, P. De Cock, et al., 1984, "Gamma-Aminobutyric Acid Transaminase Deficiency: A Newly Recognized Inborn Error of Neurotransmitter Metabolism", *Neuropediatrics*, Vol. 15, pp. 165-169.

Jones A.C., Y. Yamamura, L. Almasy, S. Bohlega, B. Elibol, J. Hubble, S. Kuzuhara, M. Uchida, T. Yanagi, D. E. Weeks and T. G. Nygaard, 1998, "Autosomal Recessive Juvenile Parkinsonism Maps to 6q25.2-q27 in Four Ethnic Groups: Detailed Genetic Mapping of the Linked Region", *American Journal of Human Genetics*, Vol. 63, pp. 80–87.

Kavaslar, G. N., S. Önengüt, O. Derman, A. Kaya and A. Tolun, 2000, "The Novel Genetic Disorder Microhydranencephaly Maps to Chromosome 16p13.3-12.1", *American Journal of Human Genetics*, Vol. 66, pp. 1705-1709.

Keats, B. J. B., J. Ott and P. M. Conneally, 1989, "Human Gene Mapping 10 - Report of the Committee on Linkage and Gene Order", *Cytogenetics and Cell Genetics*, Vol. 51, pp. 459-502.

Klein, C., M.F. Brin, P. Kramer, M. Sena-Esteves, D. de Leon, D. Doheny, S. Bressman, S. Fahn, X.O. Breakefield and L.J. Ozelius, 1999, "Association of a Missense Change in the D2 Dopamine Receptor with Myoclonus Dystonia", *Proceedings of the National Academy of Science*, Vol. 96, pp. 5173-5176.

Klein, C., L. Liu, D. Doheny, N. Kock, B. Muller, P. de Carvalho Aguiar, J. Leung, D. de Leon, S.B. Bressman, J. Silverman, C. Smith, F. Danisi, C. Morrison, R.H. Walker, M. Velickovic, E. Schwinger, P.L. Kramer, X.O. Breakefield, M.F. Brin, L.J. and Ozelius, L. J., 2002, "Epsilon-Sarcoglycan Mutations Found in Combination with Other Dystonia Gene Mutations", *Annual Neurology*, Vol. 52, pp. 675-679.

Kruglyak, L., M. J. Daly, M. P. Reeve-Daly and E. S. Lander, 1996, "Parametric and Non Parametric Linkage Analysis: A Unified Multipoint Approach", *American Journal of Human Genetics*, Vol. 58, pp. 1347-1363.

Koeppen AH and A.C. Dickson AC, 2001, "Iron in Hallervorden-Spatz Syndrome", *Pediatric Neurology*, Vol. 25, pp. 148-155.

Konakova, M., D.P. Huynh, W. Yong and S.M. Pulst, 2001, "Cellular Distribution of Torsin A and Torsin B in Normal Human Brain", *Archives of Neurology*, Vol. 58, pp. 921-927.

Lander, E. S. and D.Botstein, 1987, "Homozygosity Mapping: A Way to Map Human Recessive Traits with the DNA of Inbred Children", *Science*, Vol. 236, pp. 1567-1570.

Lathrop, G. M. and J. M. Lalouel, 1984, "Easy Calculations of Lod Scores and Genetic Risks on Small Computers", *American Journal of Human Genetics*, Vol. 36, pp. 460-465.

Leonard J.V. and A.A.M. Morris, 2000, "Inborn Errors of Metabolism around Time of Birth", *The Lancet*, Vol. 356.

Leung, J. C., C. Klein, J. Friedman, P. Vieregge, H. Jacobs, D. Doheny, C. Kamm, D. DeLeon, P.P. Pramstaller, J.B. Penney, M. Eisengart, J. Jankovic, T. Gasser, S.B. Bressman, D.P. Corey, P. Kramer, M.F. Brin, L.J. Ozelius and X.O. Breakefield, 2001, "Novel Mutation in the *TOR1A* (*DYT1*) Gene in Atypical, Early Onset Dystonia and Polymorphisms in Dystonia and Early Onset Parkinsonism", *Neurogenetics*, Vol. 3, pp. 133-143.

Medina-Kauwe, L. K., A.J. Tobin, L. De Meirleir, J. Jaeken, C. Jakobs, W.L. Nyhan, and K.M. Gibson, K. M, 1999, "4-Aminobutyrate Aminotransferase (GABA-Transaminase) Deficiency", *Journal of Inherited Metabolic Disorders*, Vol. 22, pp.414-427.

Murray, J. C., K. H. Buetow, J. L. Weber, S. Ludwigsen, T. Scherpbier-Heddema, F. Manion F, J. Quillen, V. C. Sheffield, S. Sunden and G. M. Duyk, 1994, "A Comprehensive Human Linkage Map with Centimorgan Density. Cooperative Human Linkage Center (CHLC)", *Science*, Vol. 265, pp. 2049-2054.

Nardocci N., *Infantile Neuroaxonal Dystrophy,* http://www.orpha.net/data/patho/GB/uk-INAD.pdf, 2004.

Nordli DR Jr and D.C. De Vivo, 2002, "Classification of Infantile Seizures: Implications for Identification and Treatment of Inborn Errors of Metabolism", *Journal of Child Neurology*, Vol. 3:3S3-7.

Nyholt, D. R., 2000, "All LODs are not Created Equal", *American Journal of Human Genetics*, Vol. 67, pp. 282-288.

O'Connell J.R. and D.E. Weeks, 1998, "PedCheck: A Program for Identifying Marker Typing Incompatibilities in Linkage Analysis", *American Journal of Human Genetics*, Vol.10, pp. 288.

Ott, J., 1991, *Analysis of Human Genetic Linkage*, Johns Hopkins University, Baltimore.

Ozelius, L. J., J.W. Hewett, C.E. Page, S.B. Bressman, P.L. Kramer, C. Shalish, D. de Leon, M.F. Brin, D. Raymond, D.P. Corey, S. Fahn, N.J. Risch, A.J. Buckler, J.F. Gusella, and X.O. Breakefield, 1997, "The Early-Onset Torsion Dystonia Gene (DYT1) Encodes an ATP-Binding Protein", *Nature Genetics*, Vol. 17, pp. 40-48.

Ozmen, M., M Caliskan, H.H Goebel and S. Apak, 1991, "Infantile Neuroaxonal Dystrophy: Diagnosis by Skin Biopsy", *Brain Development*, Vol. 13, pp. 256-259.

Pauls, D., 1999, "Genetic Linkage Studies, Often Among the First Steps in These Efforts, Provide a Powerful Approach to Help Elucidate the Underlying Genetic Mechanisms for Inherited Disorders", *Journal of the American Academy of Child and Adolescent Psychiatry*, Vol. 38:7, pp. 932-35.

Pellecchia, M. T., E.M. Valente, L. Cif, S. Salvi, A. Albanese, V. Scarano, U. Bonuccelli, A.R. Bentivoglio, A. D'Amico, C. Marelli, A. Di Giorgio, P. Coubes, P. Barone and B. Dallapiccola, 2005, "The Diverse Phenotype and Genotype of Pantothenate Kinase Associated Neurodegeneration", *Neurology*, Vol. 64, pp. 1810-1812.

Periquet M., B. Christoph, J.R. Lucking, V.B. Vaughan, A. Durr, G. De Michele, M.W. Horstink, M. Farrer, S.N. Illarioshkin, P. Pollak, M. Borg, C. Brefel-Courbon, P. Denefle, G. Meco, T. Gasser, M.M.B. Breteler, N.W. Wood, Y. Agid and A. Brice, 2001, "Origin of the Mutations in the Parkin Gene in Europe: Exon Rearrangements are Independent Recurrent Events, whereas Point Mutations may Result from Founder Effects", *American Journal of Human Genetics*, Vol. 68, pp. 617–626.

Pinto, D., B. Westland, G. de Haan, G. Rudolf, B. M. da Silva, E. Hirsch, Dick Lindhout, G.A. Dorothée, T. Kasteleijn-Nolst and B.P.C. Koeleman, 2004, "Genome-Wide Linkage Scan of Epilepsy-Related Photoparoxysmal Electroencephalographic Response: Evidence for Linkage on Chromosomes 7q32 and 16p13", *Human Molecular Genetics*, Vol. 14, pp. 171–178.

Rocheville, M., D.C. Lange, U. Kumar, S.C. Patel, R.C. Patel and Y.C. Patel, 2000, "Receptors for Dopamine and Somatostatin: Formation of Hetero-Oligomers with Enhanced Functional Activity", *Science*, Vol. 288, pp. 154-157.

Seven, M., A. Ozkilic and A. Yuksel, 2002, " Dysmorphic Face in Two Siblings with Infantile Neuroaxonal Dystrophy", *Journal of Genetic Counseling*, Vol. 13, pp. 465-73.

Sobel, E. and K. Lange, 1996, "Descent Graphs in Pedigree Analysis: Applications to Haplotyping, Location Scores, and Marker-Sharing Statistics", *American Journal of Human Genetics*, Vol. 58, pp. 1323-1337.

Sobel E., H. Sengul and D.E. Weeks, 2001, "Multipoint Estimation of Identity-by-Descent Probabilities at Arbitrary Positions among Marker Loci on General Pedigrees", *Human Heredity*, Vol. 52, pp. 121-131.

Sobel E., J.C. Papp and K. Lange, 2002, "Detection and Integration of Genotyping Errors in Statistical Genetics", *American Journal of Human Genetics*, Vol. 70, pp. 496-508.

Takanashi M., H. Mochizuki, K. Yokomizo, N. Hattori, H. Mori, Y. Yamamura and Y. Mizuno, 2001, "Iron Accumulation in the Substantia Nigra of Autosomal Recessive Juvenile Parkinsonism (ARJP)", *Parkinsonism and Related Disorders*, Vol.7, pp. 311-314.

Terwilliger J. D. and J. Ott, 1994, *Handbook of Human Genetic Linkage*, Johns Hopkins University, Baltimore.

Velázquez, A., M. Vela-Amieva, I. Cicerón-Arellano, I. Ibarra-González, M.E. Pérez-Andrade, Z. Olivares-Sandoval and G. Jiménez-Sánchez, 2000, "Diagnosis of Inborn Errors of Metabolism", *Archives of Medical Research*, Vol. 31, pp. 145-150.

Weissenbach, J., G. Gyapay, C. Dib, A. Vignal, J. Morissette, P. Millasseau, G. Vaysseix and M. Lathrop, 1992, "A Second Generation Linkage Map of the Human Genome", *Nature*, Vol. 359, pp. 794-801.

Zara, F., E. Gennaro, M. Stabile, I. Carbone, M. Malacarne, L. Majello, R. Santangelo, A.F. de Falco and F.D. Bricarelli, 2000, "Mapping of a Locus for a Familial Autosomal Recessive Idiopathic Myoclonic Epilepsy of Infancy to Chromosome 16p13", *American Journal of Human Genetics*, Vol. 66, pp. 1552-1557.

Zhou, B., S. K Westaway, B. Levinson, M.A. Johnson, J. Gitschier and S.J. Hayflick, 2001, "A novel Pantothenate Kinase Gene (*PANK2*) is Defective in Hallervorden-Spatz Syndrome", *Nature Genetics*, Vol. 28, pp. 345-349.

Zimprich, A., M. Grabowski, F. Asmus, M. Naumann, D. Berg, M. Bertram, K. Scheidtmann, P. Kern, J. Winkelmann, B. Muller-Myhsok, L. Riedel, M. Bauer, T. Muller, M. Castro, T. Meitinger, T.M. Strom and T. Gasser, 2001, "Mutations in the Gene Encoding Epsilon-Sarcoglycan Cause Myoclonus-Dystonia Syndrome", *Nature Genetics*, Vol. 29, pp.66-69.